

PL-TR-96-2173

REGIONAL SMALL-EVENT IDENTIFICATION USING SEISMIC NETWORKS AND ARRAYS

Michael Hedlin

Frank Vernon

J. Bernard Minster

John Orcutt

University of California, San Diego

Institute of Geophysics and Planetary Physics

La Jolla, CA 92093-0225

15 July 1996

Scientific Report No. 1

Approved for Public Release; Distribution unlimited



**PHILLIPS LABORATORY
Directorate of Geophysics
AIR FORCE MATERIEL COMMAND
HANSCOM AFB, MA 01731-3010**

DTIC QUALITY INSPECTED 8

19970108 018

SPONSORED BY
Air Force Technical Applications Center
Directorate of Nuclear Treaty Monitoring
Project Authorization T/5101

MONITORED BY
Phillips Laboratory
CONTRACT No. F19628-95-K-0012

The views and conclusions contained in this document are those of the authors and should not be interpreted as representing the official policies, either express or implied, of the Air Force or U.S. Government.

This technical report has been reviewed and is approved for publication.

Delaine Reiter
DELAINE REITER
Contract Manager
Earth Sciences Division

James Lewkowicz
JAMES F. LEWKOWICZ
Director
Earth Sciences Division

This report has been reviewed by the ESD Public Affairs Office (PA) and is releasable to the National Technical Information Service (NTIS).

Qualified requestors may obtain copies from the Defense Technical Information Center. All others should apply to the National Technical Information Service.

If your address has changed, or you wish to be removed from the mailing list, or if the addressee is no longer employed by your organization, please notify PL/IM, 29 Randolph Road, Hanscom AFB, MA 01731-3010. This will assist us in maintaining a current mailing list.

Do not return copies of this report unless contractual obligations or notices on a specific document requires that it be returned.

REPORT DOCUMENTATION PAGE

Form Approved
OMB No. 0704-0188

Public reporting burden for this collection of information is estimated to average 1 hour per response, including the time for reviewing instructions, searching existing data sources, gathering and maintaining the data needed, and completing and reviewing the collection of information. Send comments regarding this burden estimate or any other aspect of this collection of information, including suggestions for reducing this burden, to Washington Headquarters Services, Directorate for Information Operations and Reports, 1215 Jefferson Davis Highway, Suite 1204, Arlington, VA 22202-4302, and to the Office of Management and Budget, Paperwork Reduction Project (0704-0188), Washington, DC 20503.

			3. REPORT TYPE AND DATES COVERED Scientific No. 1
1. AGENCY USE ONLY (Leave blank)	2. REPORT DATE 15 July 1996	4. TITLE AND SUBTITLE Regional small-event identification using seismic networks and arrays	
6. AUTHOR(S) Michael Hedlin, Frank Vernon, J. Bernard Minster, John Orcutt			5. FUNDING NUMBERS F19628-95-K-0012 PE35999F PR 5101 TA GM WU AF
7. PERFORMING ORGANIZATION NAME(S) AND ADDRESS(ES) University of California, San Diego Scripps Institution of Oceanography IGPP 0225 La Jolla, CA 92093-0225			8. PERFORMING ORGANIZATION REPORT NUMBER
9. SPONSORING/MONITORING AGENCY NAME(S) AND ADDRESS(ES) Phillips Laboratory 29 Randolph Road Hanscom AFB, MA 01731-3010			10. SPONSORING/MONITORING AGENCY REPORT NUMBER PL-TR-96-2173
Contract Manager: Delaine Reiter/GPE			
11. SUPPLEMENTARY NOTES			
12a. DISTRIBUTION AVAILABILITY STATEMENT Approved for public release; distribution unlimited			12b. DISTRIBUTION CODE
13. ABSTRACT (Maximum 200 words) The CTBT negotiations have endowed small seismo/acoustic events (mb ~ 2.5) with a much greater significance than they have had in the past and have increased the need for automated regional discrimination. We have been contracted by AFTAC to develop a small event discriminant that uses a time-frequency expansion (sonogram) of seismic coda to discriminate ripple-fired mining explosions from single explosions and earthquakes. The Automated Time-Frequency Discriminant (ATFD) which we have developed uses a binary sonogram which is derived from the original, spectral, sonogram by the application of filters which replace the spectral information with a binary code which simply reflects local spectral highs and lows. We have found that the binary patterns which we extract from the coda of ripple-fired events are banded and thus distinct from those obtained from single explosions and earthquakes. The bands, which result from source finiteness, intershot delays or a combination of the two, are largely independent of time and of the recording component. The ATFD uses three statistical tests to measure the time- and recording component-independence and automatically recognize these bands. All of the raw discrimination parameters produced by these tests are merged into a single discriminant score with multivariate statistics.			
14. SUBJECT TERMS CTBT, Time-frequency expansion, Wavelets, Automated Discrimination, Multivariate statistics, Coda cepstrum, Ripple-firing, Binary sonogram			15. NUMBER OF PAGES 40
			16. PRICE CODE
17. SECURITY CLASSIFICATION OF REPORT Unclassified	18. SECURITY CLASSIFICATION OF THIS PAGE Unclassified	19. SECURITY CLASSIFICATION OF ABSTRACT Unclassified	20. LIMITATION OF ABSTRACT SAR

ABSTRACT

The CTBT negotiations have endowed small seismo/acoustic events ($\text{mb} \sim 2.5$) with a much greater significance than they have had in the past and have increased the need for automated regional discrimination. We have been contracted by AFTAC to develop a small event discriminant that uses a time-frequency expansion (sonogram) of seismic coda to discriminate ripple-fired mining explosions from single explosions and earthquakes. The Automated Time-Frequency Discriminant (ATFD) which we have developed uses a binary sonogram which is derived from the original, spectral, sonogram by the application of filters which replace the spectral information with a binary code which simply reflects local spectral highs and lows. We have found that the binary patterns which we extract from the coda of ripple-fired events are banded and thus distinct from those obtained from single explosions and earthquakes. The bands, which result from source finiteness, intershot delays or a combination of the two, are largely independent of time and of the recording component. The ATFD uses three statistical tests to measure the time- and recording component-independence and automatically recognize these bands. All of the raw discrimination parameters produced by these tests are merged into a single discriminant score with multivariate statistics.

During the past year we have tested the ATFD on data collected by single stations, arrays and regional networks in central Asia, Europe and North America. We have found the automated discriminant to be robust, with misclassification probabilities ranging from 0.5 to 3.5 percent. The method is easily adapted to any kind of regional seismic data. No expert analysis of the time-frequency patterns is required.

To improve the ATFD we have analyzed wavelet expansions of coda. We have found that wavelets are capable of much higher resolution in time than is possible with a multitaper-sonogram expansion. We are currently using a new bias-minimizing wavelet technique (*Lilly & Park, 1995*) to process 3-component data and analyze the evolution of spectral amplitude and polarization with time and frequency and improve our understanding of ripple-fired coda. We intend to determine if a low frequency spectral signature (perhaps caused by source finiteness) might be used for discrimination at far-regional distances. We have conducted a preliminary survey of discrimination at low frequencies using the Kazakh NRDC network.

We have begun to look at discriminants based on hybrid (seismo/acoustic) data and will shortly collect data to help us address the issue of outliers. These data will be collected this summer in Wyoming and will consist of broadband seismic, acoustic and infrasound recordings of ground truthed mining explosions in the Black Thunder coal mine. With this experiment we will also be examining the utility of continuous GPS for event detection. At regional distances from the Black Thunder mine we will deploy a network of 3 continuous GPS receivers and will use the data to look for ionospheric perturbations resulting from the near-vertical acoustic emissions.

Keywords: comprehensive test ban treaty (CTBT), time-frequency expansion, wavelets, automated discrimination, multivariate statistics, coda cepstrum, ripple-firing, binary sonogram.

A. OBJECTIVES/PROGRESS

(1) OBJECTIVES

During the term of our existing contract we will expand significantly research we have conducted into the small-event discrimination problem. Our interest has been in using the spectral characteristics of whole regional waveforms to discriminate ripple-fired from non-ripple-fired events (incl. earthquakes and single-event explosions). Our objectives are to apply our automated whole waveform time-frequency discriminant (ATFD) to large event populations in varied data sets to test transportability and robustness and to enhance the ATFD with more sophisticated processing. In specific we have the following objectives:

1.1 Robustness and transportability

Apply our existing ATFD (Hedlin et al., 1990) to a number of dissimilar, well separated, regional data sets with large populations of ripple and non-ripple-fired events to gauge robustness and regional dependence. We will apply the technique to vertical component data from several networks and arrays using low (1 to 20 Hz) and broad (1 to 100 Hz) frequency bands. Particular attention will be paid to the cause of outliers. We will determine the extent to which array data can suppress noise and increase the range of the ATFD.

1.2 Software development

Enhance the ATFD via (1) wavelet analysis, (2) more advanced spectral analysis techniques [e.g. the statistics of Higher Order Crossings (HOC)], (3) advanced processing techniques to permit full use of modern three-component (3C) networks and arrays. 3C data sets examined under objective 1.1 will be re-analyzed to assess improvement.

1.3 Comparisons with other techniques

Analyze the same data sets, discussed under objective 1.1, with a complementary technique (e.g. a “regionally trained” spectral ratio method) to assess relative capabilities under different settings. Our intent is to develop a complementary technique that might be merged through evolutionary programming with our own to provide a more comprehensive, multivariate, discriminant. The time-frequency approach, taken alone, will not discriminate between single-event explosions and earthquakes.

1.4 Low-frequency discrimination

Address the question of what low frequency (e.g. 1 to 20 Hz) time-independent signature should be produced by mines that use short (e.g. 20 ms) delays especially when delay times are irregular. Use any available “ground truth” data to explain any modulations observed at low frequencies and test the theory that they might be due to temporal finiteness of the source (Hedlin et al., 1990).

1.5 Contribution of software to database accessing systems

Develop algorithms that are designed to operate on the CSS 3.0 database structure and will be available to all interested parties.

(2) PROGRESS

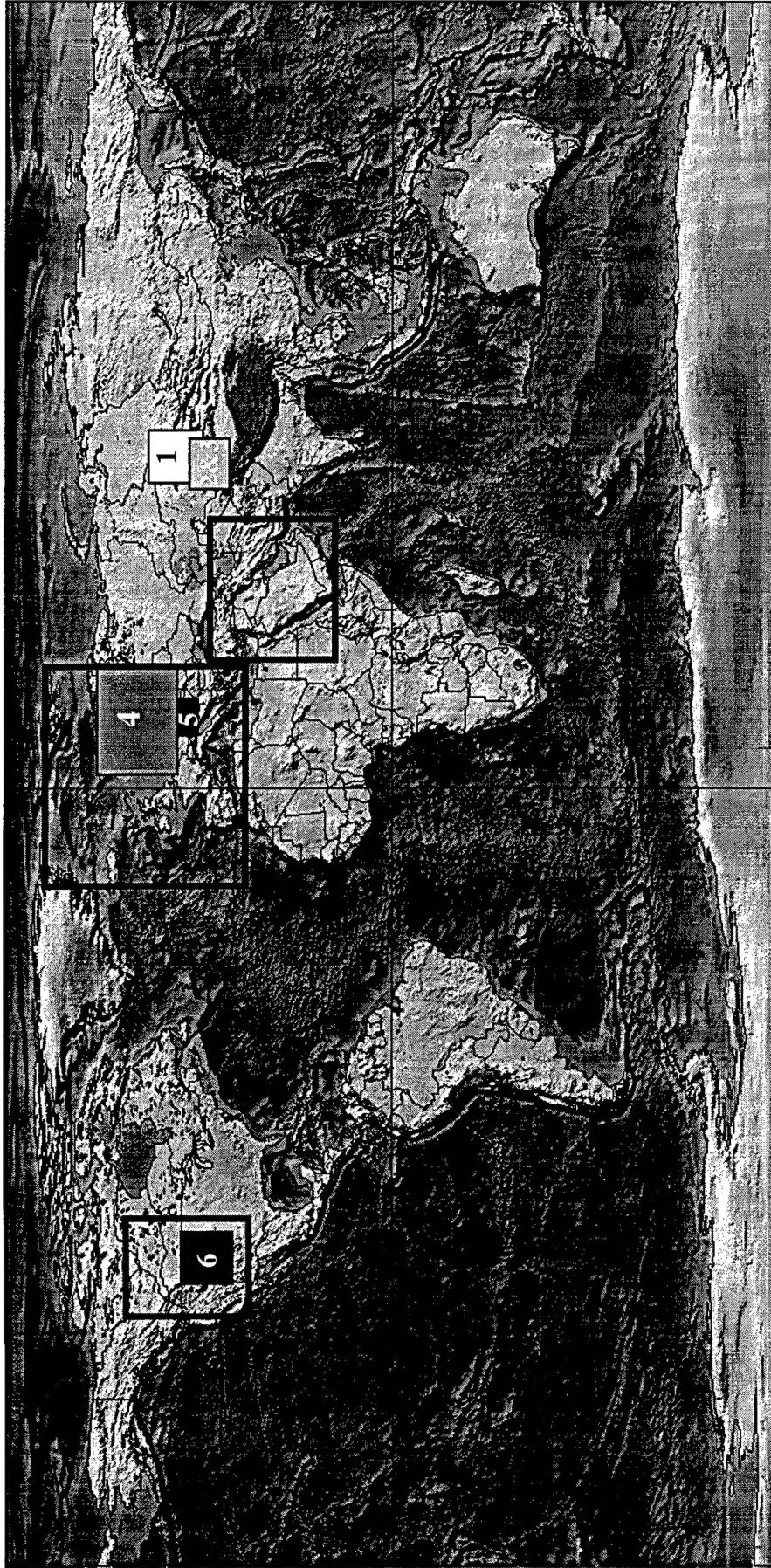
The automated time-frequency discriminant. Under previous Air Force contracts (F19628-87-K-0013 and F19628-88-K-0044) we developed a discriminant that seeks long-lived spectral modulations in major seismic phases and coda. Long lived modulations can be produced by seismic resonance and by ripple firing. We expand time series into time-frequency displays (sonograms) to search for these patterns. *Hedlin et al (1989)* developed a procedure whereby a binary sonogram is derived from the original, spectral, sonogram by the application of filters which replace spectral information with a binary code which simply reflects local spectral highs and lows. *Hedlin et al. (1990)* produced a procedure to automatically recognize time independent patterns. This technique utilizes a two-dimensional Fourier transform of the binary sonogram which reveals the dependence of the binary pattern on frequency and time. In view of its resemblance to the cepstrum (which identifies periodicities in single spectra), and the fact that it is derived from onset and coda phases we now refer to it as the coda cepstrum (*Hedlin et al., 1995*).

Hedlin et al. (1989) also noted that the modulations were remarkably independent of the recording direction. As an example of this we display, in figures 1, 2, and 3, a summary of an analysis of recordings of earthquakes and quarry blasts made by the KNET in Kyrgyzstan. Examining the quarry blasts (located just northeast of CHM) and the earthquakes located to the southwest of the network we found that the network average cross correlations of the binary patterns between the recording components (average of EW vs Z, Z vs NS and EW vs NS) clearly separate quarry blasts from earthquakes. A second set of earthquakes (the cluster located within the network) and a second set of quarry blasts from the same mine have essentially the same separation (Figure 3).

The current Automated Time Frequency Discriminant (now known as the ATFD) recognizes long lived modulations by applying three separate tests. The algorithm estimates the time-independence of the binary patterns by calculating the autocorrelation of individual narrow band (single frequency) timeseries. The “bandedness” is estimated by calculating the coda cepstrum and taking the extreme value which is independent of time. Independence from recording direction is judged by cross-correlation. These individual parameters are merged into a single discrimination score with the aid of multivariate statistics (*Seber, 1984*). The means by which the binary sonograms are reduced to a few discrimination parameters is reviewed in Appendix A of this report.

Global test of the ATFD. We have used a wide variety of datasets to test the utility of the ATFD. Specifically, we have tested the adaptability of the algorithm to various styles of seismic deployment (*incl.* single 3-Component stations, single- and 3-Component networks and arrays) varying seismic instrumentation (*incl.* short period and broadband), different geologic settings and mining practice. In the past year we have analyzed the following datasets (Figure 1):

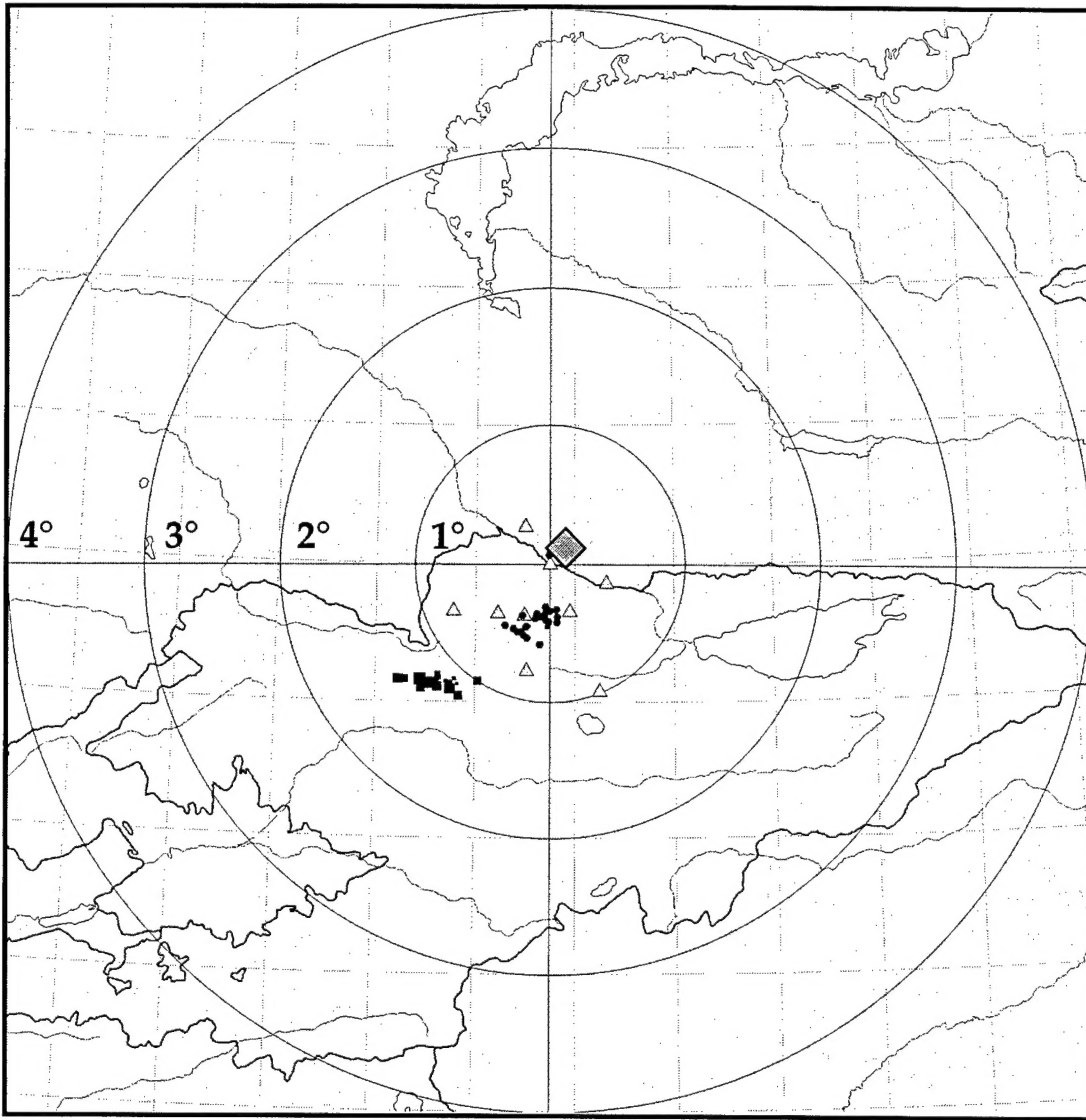
- 1) single (chemical) explosions and quarry blasts recorded by a sparse 3-Component network (NRDC) deployed in 1987 on a high Q crust in central Kazakhstan. The events occurred within 300 km of the stations. Event identification was based on C. Thurber's interpretation of SPOT photos (*Thurber et al., 1989*) and the fact that the Kazakh platform is seismically quiet.
- 2&3) earthquakes and quarry blasts recorded by a dense (10 stations in an aperture of 200 km) telemetered 3-Component broadband network (KNET) deployed in Kyrgyzstan between



Etopo5 basemap courtesy of
[http://www.geo.cornell.edu/geology/
me_na/dataset_info/new_etopo5.html](http://www.geo.cornell.edu/geology/me_na/dataset_info/new_etopo5.html)

Figure 1 Locations of the datasets analyzed in the past year. Datasets 1, 4, 5 and 6 are NRDC, NORESS A, Vogiland (GERESS) and Carlin (respectively) and are all reviewed in appendix B. Datasets 2 and 3 are KNET A and B, both reviewed in the main text (Figures 2 through 8). The open boxes indicate regions which we will examine in the coming year.

KNET A and B - A dense 3C network



◆ Mine

Figure 2. The 10 station Kyrgyz telemetered broadband network (grey triangles). Two clusters of earthquakes are contrasted with two separate sets of quarry blasts which occurred in a mine located just northeast of the station CHM (at the crosshairs). The remote set of events (dataset "A") are aftershocks to the magnitude 7.4 Suusamyr thrust earthquake. The second set of earthquakes (dataset "B") occurred within the network, roughly 50 km south of CHM.

the Kazakh platform to the north and the seismically active Tien Shan to the south. We have analyzed two clusters of earthquakes and contrasted them with two sets of quarry blasts which occurred at the same mine (Figure 2). The limestone mine was located by Rob Mellors (UCSD) at 43.028° N and 74.888° E. Events were determined to be quarry blasts on the basis of their location and the origin time - the limestone shots typically occurred in the late afternoon. In addition some of these events produced obvious acoustic signals which arrived at CHM roughly 37 s after P . The network made triggered recordings at 100 sps and continuous recordings at 20 sps.

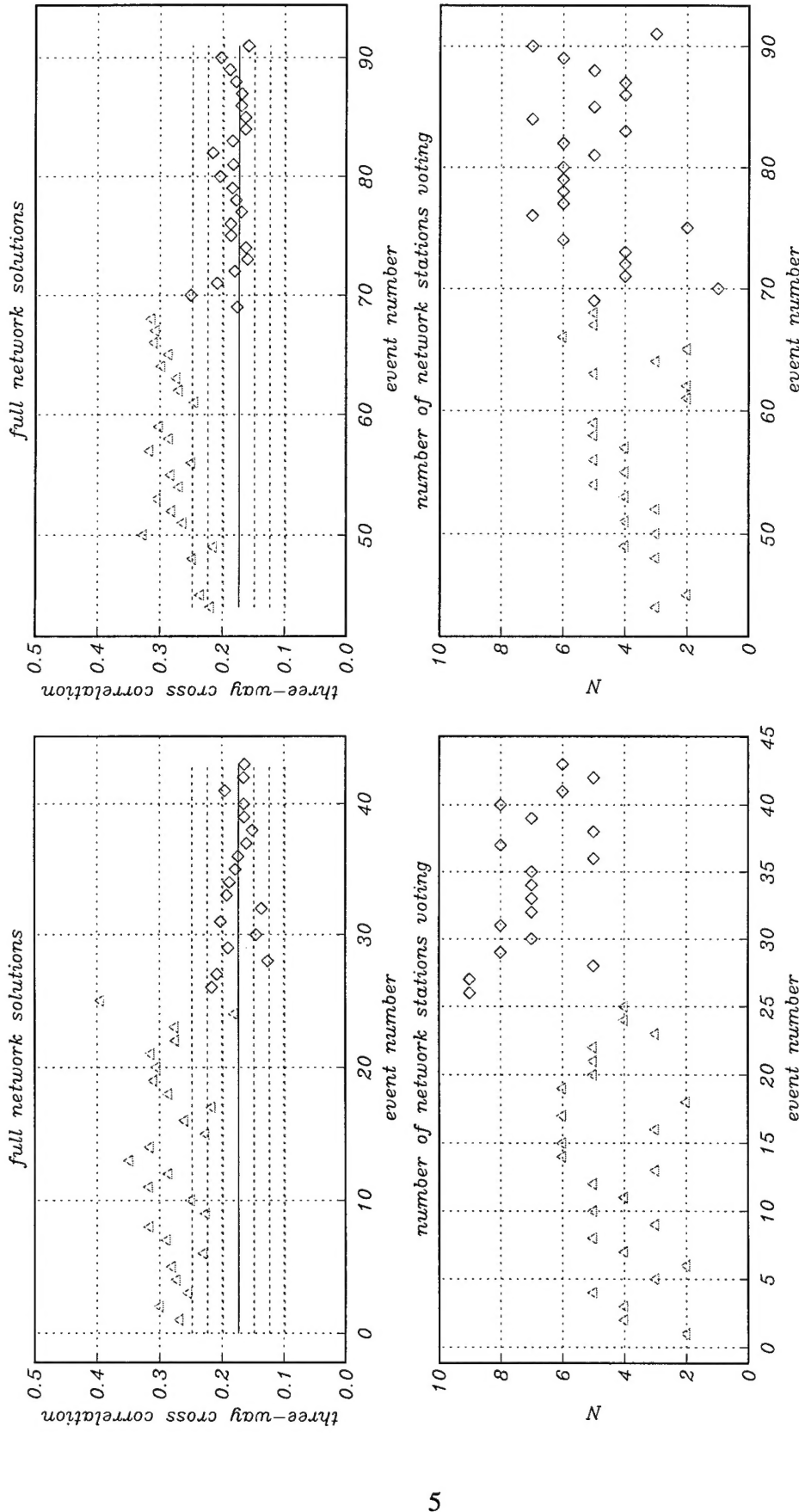


Figure 3 Full network averaged three-way crosscorrelations calculated using the events in dataset A (left figures) and B (right). We find that the network solutions exhibit little crossover between the two event types. Using the earthquakes in dataset A we have calculated a mean and +/- 1,2 and 3 standard deviations. These statistics are overlain on the network solutions from dataset B showing that the cross-correlations of the two sets of events are essentially the same.

- 4) recordings of quarry blasts and earthquakes made by the NORESS small aperture array in southern Norway. NORESS is comprised of 25 stations of GS13 seismometers in a 3 km aperture on Precambrian or Paleozoic hard-rock. Four of the stations have 3-Components. The signals are digitized at 40 sps. The events in this dataset occurred within 7.5° of the array.
- 5) recordings of quarry blasts and earthquakes made by GERESS (a NORESS style array in Germany). These recordings were obtained from the European Ground Truth Database and were contributed by J. Wuster. The earthquakes largely occurred in swarms. The quarry blasts occurred in Western Bohemia (*Wuster, 1993*).
- 6) recordings of quarry blasts (in the Newmont Gold Mine) and earthquakes (including events in the Rock Valley earthquake sequence near NTS) made by a single 3-Component station (ELK in the LNN network) located near Carlin, NV roughly 80 km from the mine. This hard rock mine (which detonates ripple-fired shots every 2 days each using 15 to 100 tons of explosives) has been monitored by LLNL scientists (incl. Drs. Peter Goldstein, Bill Moran and Steve Jarpe). Mining records have been used to constrain the blast patterns, which typically involve delays from 50 to 100 ms. These data were provided by LLNL.

The ATFD tested on a dense 3-Component network: To illustrate the technique we show the results of the analysis of the second and third datasets (collected by KNET; Figures 1 and 2). The upper two and lower left panels of Figures 4 and 5 we show the raw output from the ATFD (refer to appendix A for details). These panels show how well the two event types (earthquakes and quarry blasts) are separated by the metrics applied to the time-frequency expansions. The lower right panel shows the linear discriminant scores obtained by a multivariate analysis of the raw parameters. Considering dataset A we found that two events (of 47) were misclassified. This is not likely due to poor coverage, since one of the events was recorded by 9 stations (Figure 6), but likely was due to the source or propagation. As discussed by *Hedlin et al. (1989)* a time independence can be acquired through propagation by resonance. As discussed by numerous authors (incl. *Stump et al., 1994*) ripple fired shots will, sometimes, not produce scalloped spectra. Outliers, such as these, are a critical problem and are discussed in more detail later in this report.

The results of the KNET analysis, and the other studies summarized above, are shown in Figure 7 where we show the misclassification probabilities (see Appendix B for a full description of these analyses). By necessity we have paid the closest attention to the problem of discriminating quarry blasts from earthquakes. We expect that earthquakes should not yield coda with time- or component-independent spectral qualities and thus have used them to serve as proxys for single explosions. However, the most challenging and interesting problem involves the discrimination of single and multiple explosions. Although we haven't analyzed a large number of single explosions (3 recorded by the NRDC network in Kazakhstan; dataset # 1) it appears that the ATFD is effective at separating these event types (see *Hedlin et al., 1995* for details). To further address this problem we will examine the single explosions recorded during the 1995 Black Thunder experiment (*Stump et al., 1995; Pearson et al., 1995*).

A discriminant based on a wavelet expansion: In the preceding sections we analyzed time series using multitaper spectral estimation (*Thomson, 1982*). using data selected by a simple sliding window. While this approach takes advantage of multitaper's proven ability to yield minimally biased spectral estimates from short time series and has proven useful for discrimination it has several drawbacks. The

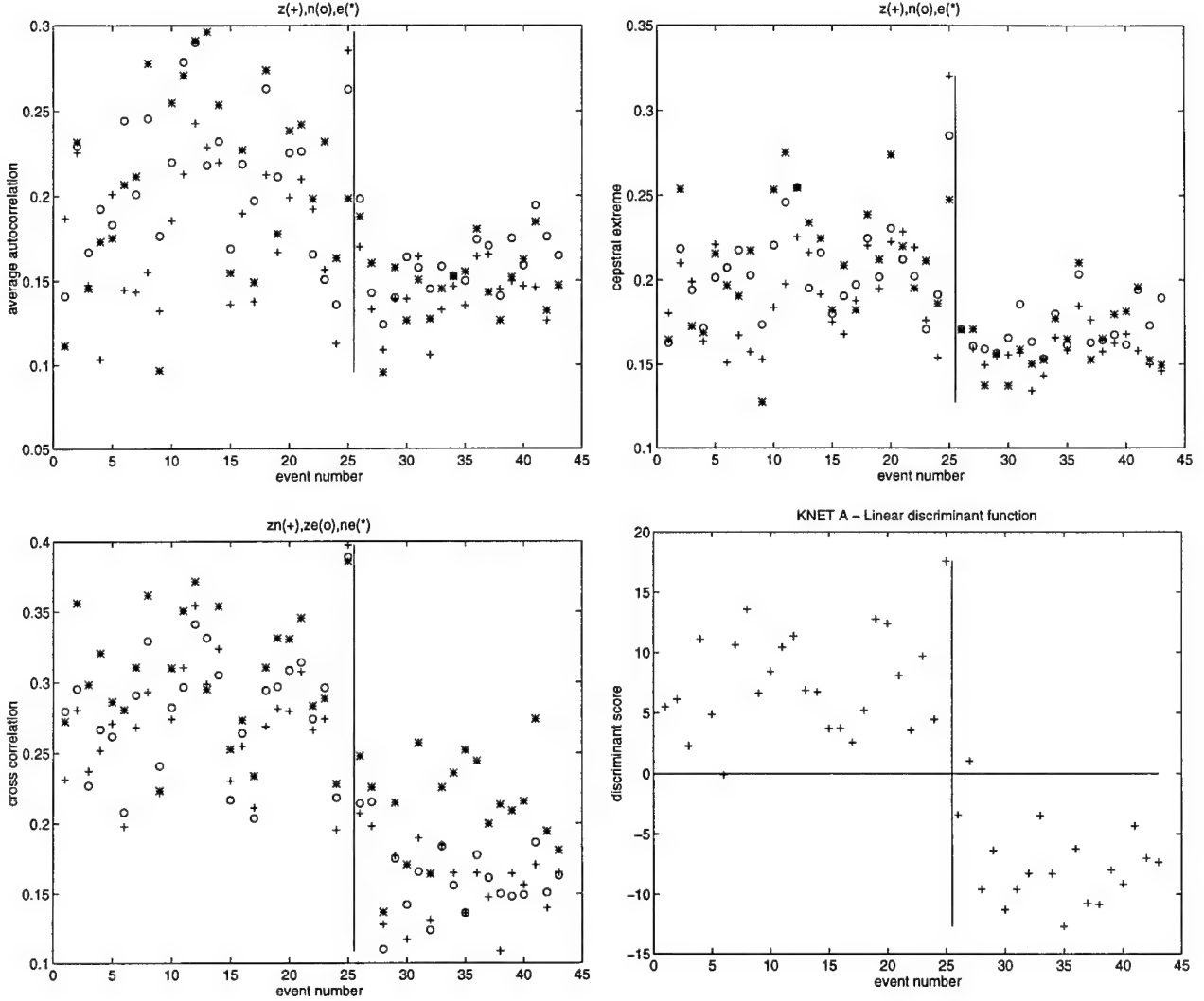


Figure 4. KNET A, The current ATFD yields 3 types of discrimination parameters - all of which are defined in Appendix A. One, shown in the lower left panel, based on the network average cross-correlation across the three recorded channels, is similar to that presented in the preceding figures. A value of 1 indicates that the three pairs of binary sonograms are perfectly correlated at all stations. The parameter which is based on the autocorrelation of single frequency timeseries, is shown in the upper left panel. A value of 1.0 means that all frequencies at all stations are invariant wrt time (they have either +1 or -1 at all times). The third, based on the coda cepstrum (see *Hedlin et al., 1989; 1995*), is shown in the upper right. A binary sonogram which is periodic in frequency and independent of time would have an extreme value of 1.0. All three of these discriminants show good separation between the two types of events in dataset A. The linear discriminant scores, obtained through multivariate statistics, are shown on the lower right.

resolution in time-frequency expansions based on sliding window ffts is invariant with-respect-to time and frequency. Typically parameters used to calculate these sonograms are chosen in an *ad hoc* fashion.

An alternate means to expand a time series into a time-frequency plane is based on wavelets (*Daubechies, 1990*). A wavelet transform does not fix the tradeoff between time and frequency localization by fixing the time window. Instead it allows the time and frequency resolution to vary inversely to one another

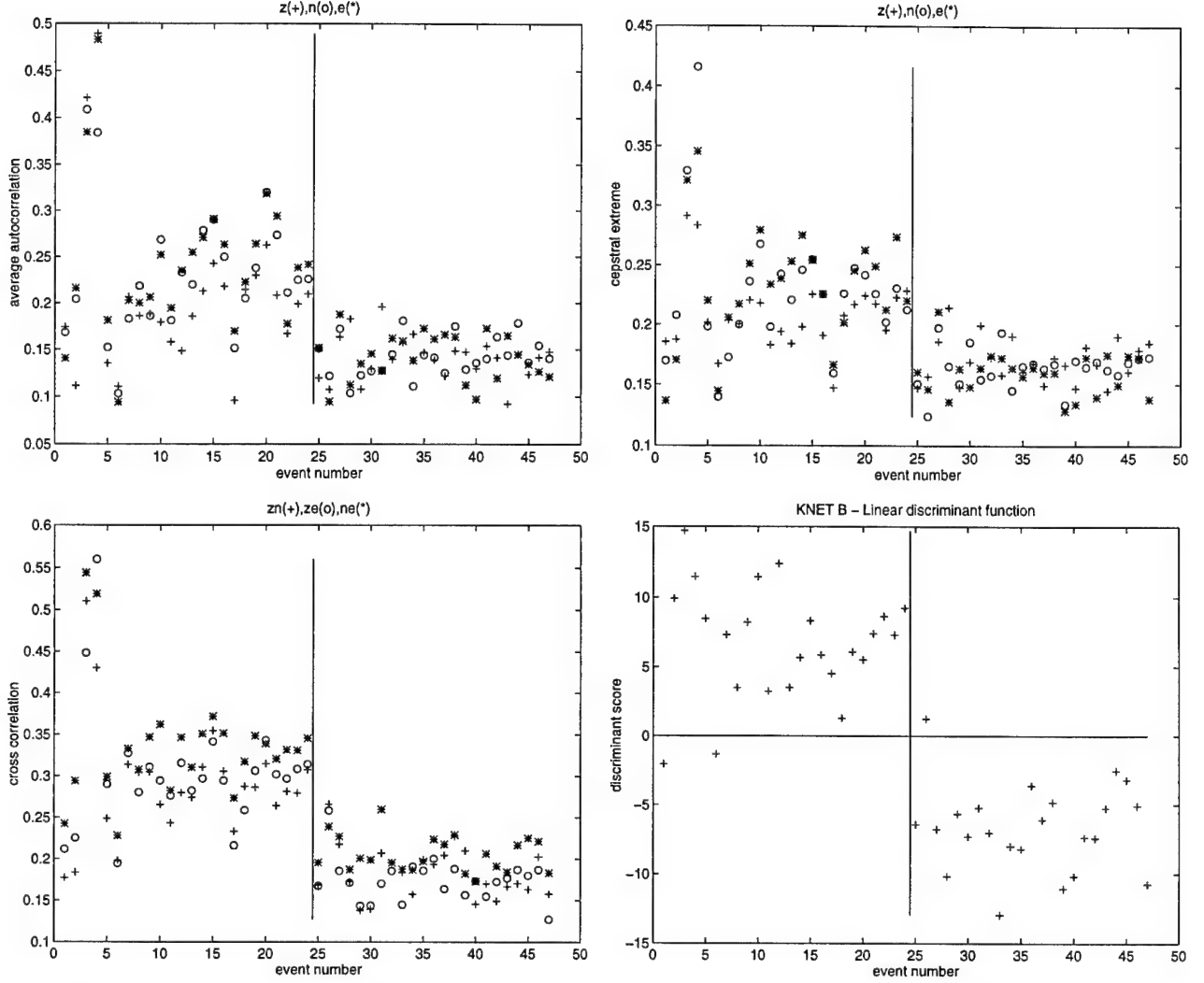


Figure 5. The same as Figure 4 except this figure shows results from the events in KNET dataset B.

as it traverses the time series. The wavelet transform has been shown to be particularly useful in the analysis of waveforms beset with both abrupt changes in time and narrow, highly-concentrated frequency bands (similar in concept to the tapers used in multi-taper analysis) which can be used together to yield low-variance time and frequency representations of spectral power and polarization. Three wavelets (calculated assuming a time-bandcenter product of 3.0, a time-bandwidth product of 2.5, an analysis frequency of 5.0 Hz) are shown in Figure 8.

To illustrate the potential power of wavelets we consider multitaper and multiwavelet expansions of a controlled signal. We use the recording of a calibration explosion made by the NRDC station BAY (see Appendix B) as an empirical Green's function and, assuming linear superposition, synthesize a quarry blast waveform where the quarry blast consists of 5 shots spaced at 50 ms (Figure 9). As expected the synthetic sonogram has a time-independent spectral high at 20 Hz (the 40 Hz overtone is at noise level). In Figure 10 we show the multitaper sonogram and time series of 16 seconds including the P wave onset and early coda from the calibration explosion. The same portion of the synthetic is displayed in the middle figure. The time-bandwidth product used was 4 yielding a frequency resolution of

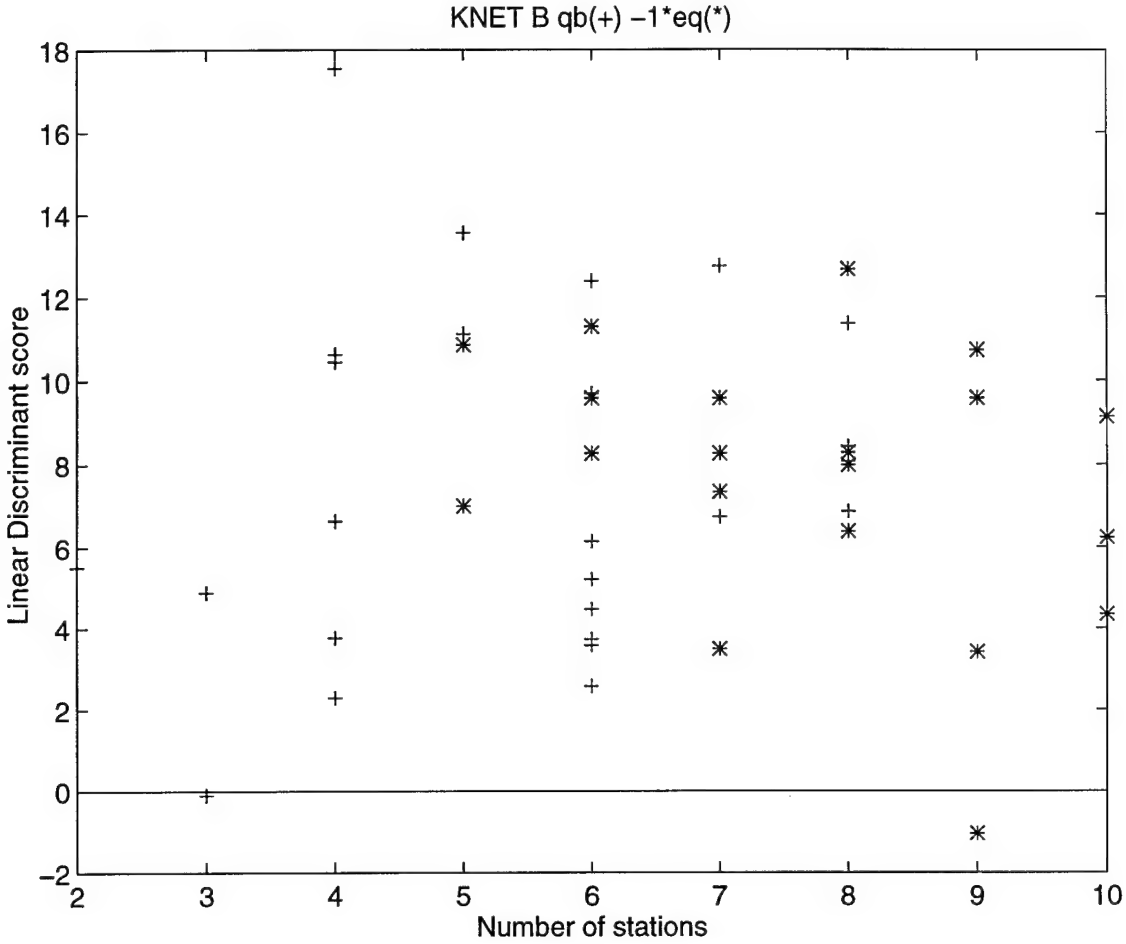


Figure 6. Considering KNET dataset A events we plot the linear discrimination scores plotted against the number of stations used (the earthquake scores have been multiplied by -1 so that all symbols appearing below the solid line - at zero - represent misclassifications). We find that one earthquake recorded by 9 stations failed the test. A quarry blast recorded by 3 stations was also misclassified.

4 Hz. In the right panel (Figure 10) we display a multiwavelet transform of the synthetic quarry blast time series. While this expansion has roughly the same frequency resolution as provided by the multitaper approach the time resolution is much greater. At 20 Hz the wavelet spans 0.5 seconds.

Outliers and Hybrid monitoring: The Black Thunder seismo/acoustic experiment. To improve the science of small-event discrimination we need to understand better why some events are misclassified and we need to explore better data collection and processing techniques. To investigate the physical relationship between the ripple-fired source and regionally recorded seismic and acoustic wavefields we have formed a collaboration with Brian Stump, Craig Pearson and Rod Whitaker at LANL. The primary result of this collaboration is an experiment which will occur in July and August of this year. As part of this experiment Brian Stump and Craig Pearson from LANL will deploy video equipment, accelerometers and acoustic gauges inside the Black Thunder coal mine in the Powder River Basin of Wyoming. The Powder River Basin includes some 18 coal mines which, in total, generate an average of 1 mine-blast every other day. The in-mine equipment will record not just the timing of the shots (t) in the mine but also the horizontal spatial positions (x and y).

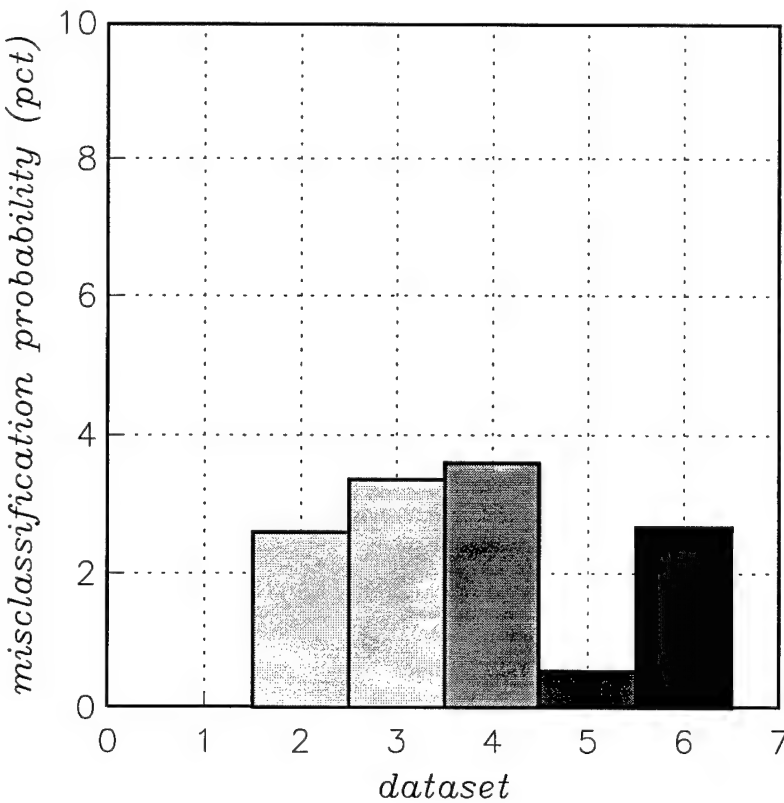


Figure 7. Misclassification probabilities in the datasets described in Figure 1 and reviewed in the main text and in Appendix B. Dataset 1 (NRDC) contains recordings of quarry blasts and just 3 single-explosions and is not summarized statistically. Datasets 2 and 3 (KNET A and B) are reviewed in detail in the main text.

acoustic and infrasound equipment to assess the signal to noise gain that the infrasound receivers (loaned to us by Rod Whitaker) will give us. The acoustic and seismic equipment will be co-located to allow us to assess the value of a seismo/acoustic station. The acoustic instrumentation should be located within the first acoustic convergence zone and we expect the signals from the mine will be relatively strong to the west due to refraction in the mid-atmosphere. All acoustic signals will be digitized at 40 sps.

A second team from UCSD will deploy 3 continuous GPS receivers to detect ionospheric perturbations that result from the pressure front that emanates from the mine and is not ducted between the mid-atmosphere and the ground but propagates into the ionosphere. The current plan has 2 receivers located near to each other at a range of 50 km to the southwest of the mine. A third receiver will be deployed on the same azimuth but at a range of 200 km (Figure 11).

In addition to this near-regional equipment we have made arrangements with Bob Ellis and Michael Bostock (both at the University of British Columbia) to collect far-regional recordings of the mine blasts at 700 km (using an array of 7 seismic sensors in Saskatchewan, Canada) and at 2000 km (using an array of seismic sensors located in the Northwest Territories, Canada). We have also made arrangements with Jim Zollweg (Idaho) and Scott Smithson (Wyoming) for additional, near- to mid-regional recordings.

A team from UCSD will deploy a regional network of broadband seismometers, pressure gauges and infrasound receivers (Figure 11). The network will include five 3-Component broadband seismic stations (STS2's) sampling continuously at 100 sps. Four of the stations will be located 200 km from the mine. The fifth station will be deployed 100 km from the mine on the same azimuth as one of the outer stations. This temporary network will add to permanent seismic deployments that include the 3-Component GSETT3 beta station RSSD and the array at Pinedale. Three pressure gauges will be deployed at the stations located 200 km to the north, south and west of the mine. Paired with the pressure gauge at the western site will be a small infrasound array consisting of 3 infrasound receivers in a triangle 100 m on a side.

In part we will be pairing the

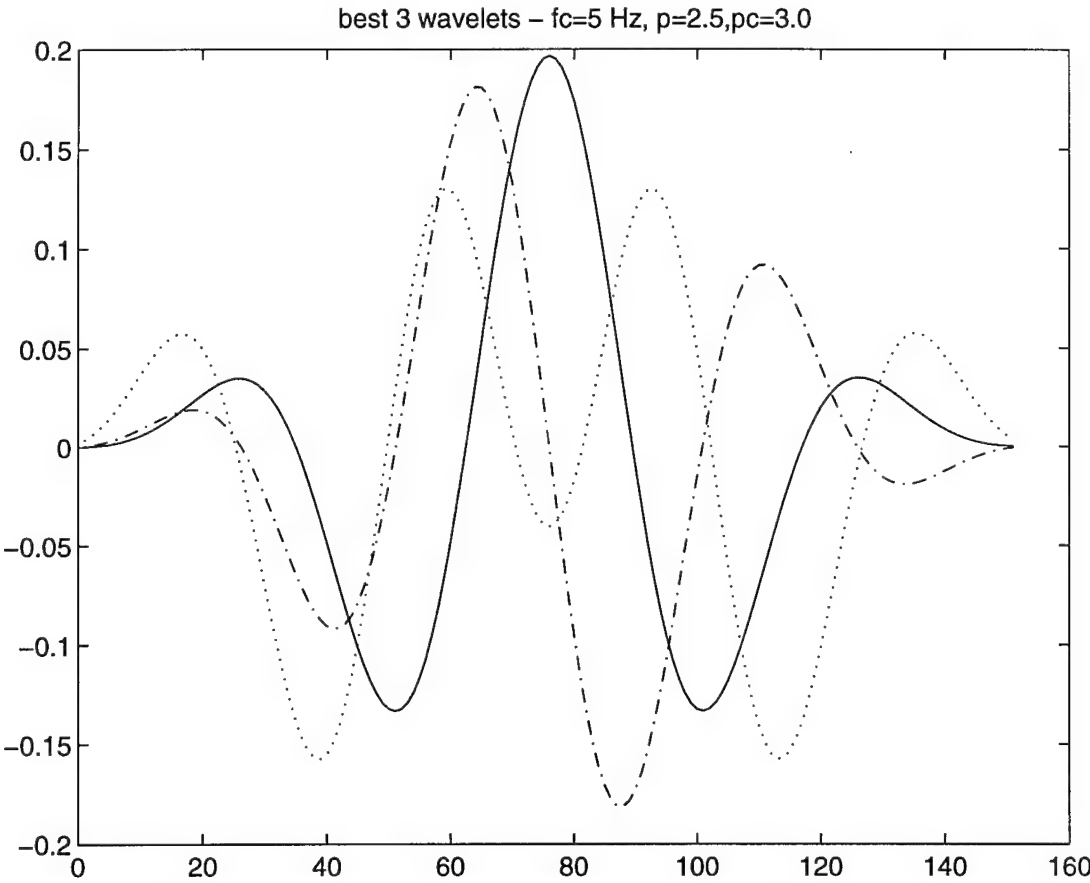
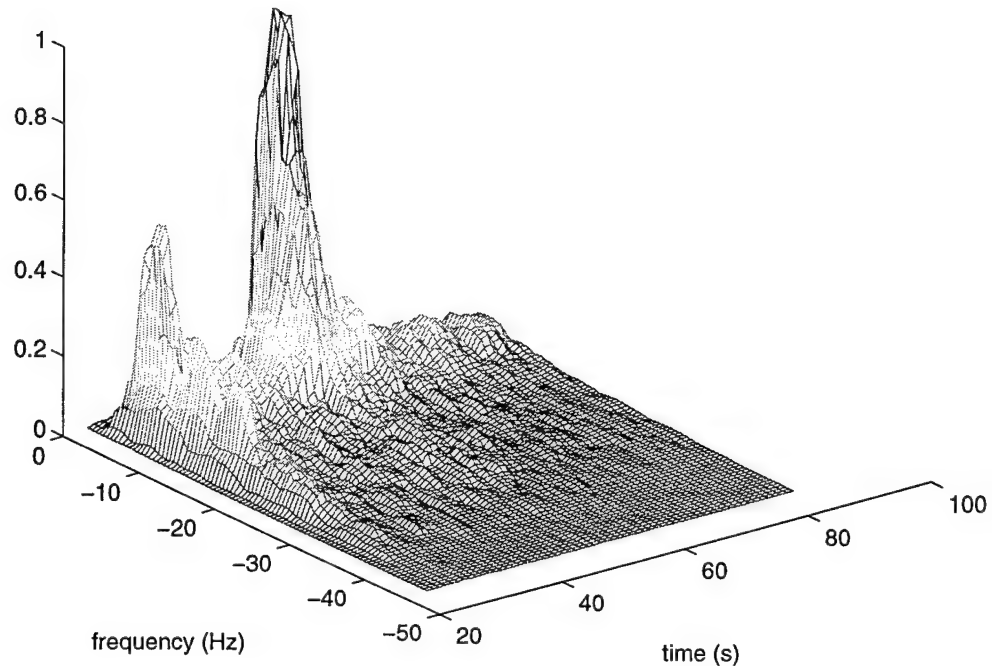


Figure 8. The three best bias minimizing wavelets calculated with a bandcenter product of 3.0; a time-bandwidth product of 2.5 and an analysis frequency of 5.0 Hz.

We expect that this instrumentation will record four significant (cast) explosions. On July 19 there will be a shot involving ~4 million pounds of explosives. We expect two additional shots (3 to 4 million pound range) to occur the week of July 29 with a fourth occurring in mid August. The proximity of this mining activity with regional earthquakes located in the Intermountain Seismic Belt to the west of Pinedale (*Hansen, 1992*) should provide a number of natural event records. The data from this experiment will allow us to test the utility of pressure gauges and an infrasound array to detect acoustic emissions from a surface mine and estimate the back azimuth to the source. We will also be testing the utility of the hybrid seismo/acoustic monitoring station and have an opportunity to address the issue of outliers. The video data that Brian and Craig collect will enable us to model the regional waveforms and should allow us to test linear superposition at four azimuths. Permanent stations and the temporary deployments in Canada will allow us to determine the effective range of the ATFD. In total we hope to be able to answer the following questions: 1) Can earthquakes give rise to time-independent modulations?; (2) Under what circumstances will ripple-fired events not yield modulated spectra?; (3) To what extent is success dependent on source-receiver range and azimuth? Using linear superposition theory we will predict the time independent spectral signature that should be present in mine records. Using our multi-taper sonogram algorithm (*Hedlin et al., 1989*) we will expand the 3-component recordings into time-frequency displays and investigate the correspondence between the expected and observed time independent signatures.

Chemex 2 recorded at BAY.C0



Synthetic quarry blast – 5x50 ms delays

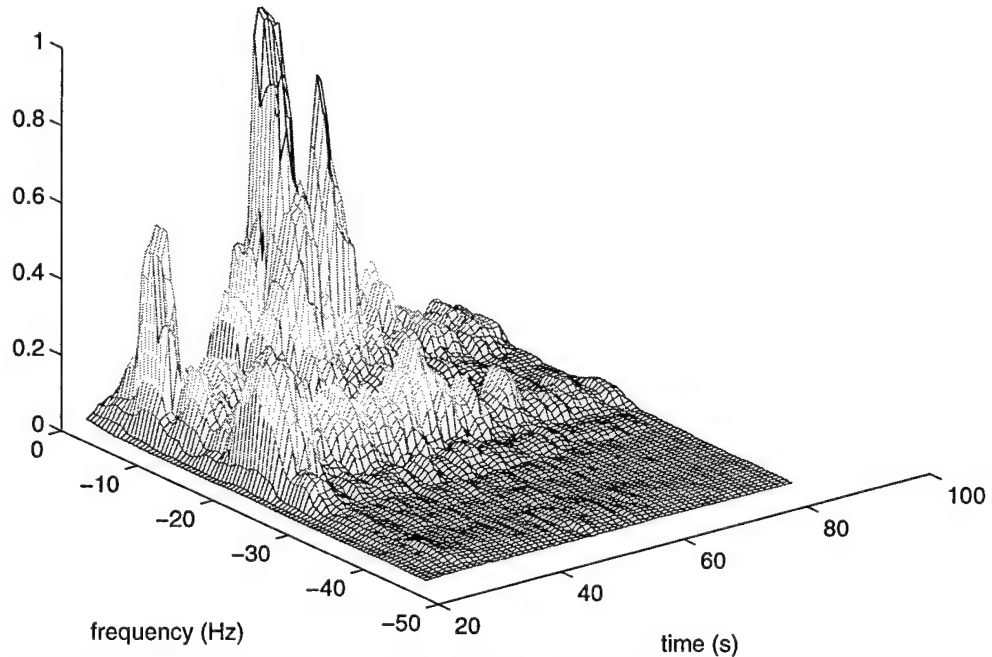


Figure 9. A sonogram calculated from a calibration (single) chemical explosion recorded by the NRDC network station BAY (see Appendix B) is shown on top. On the bottom we show the sonogram of a synthetic quarry blast which comprises 5 shots spaced evenly at 50 ms.

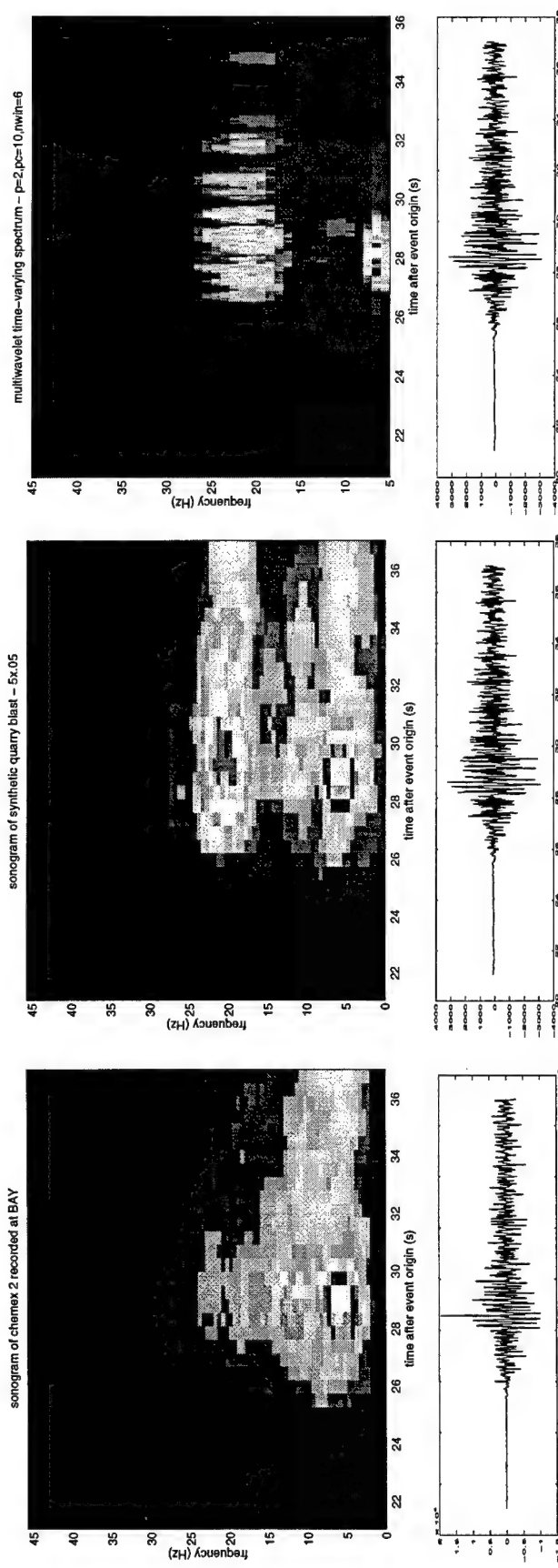


Figure 10. Sonograms of the calibration explosion (left) and the synthetic quarry blast (middle). The wavelet expansion of the synthetic quarry blast is shown on the right. Note the much higher time-resolution in the wavelet transform.

WY96 Regional Deployment

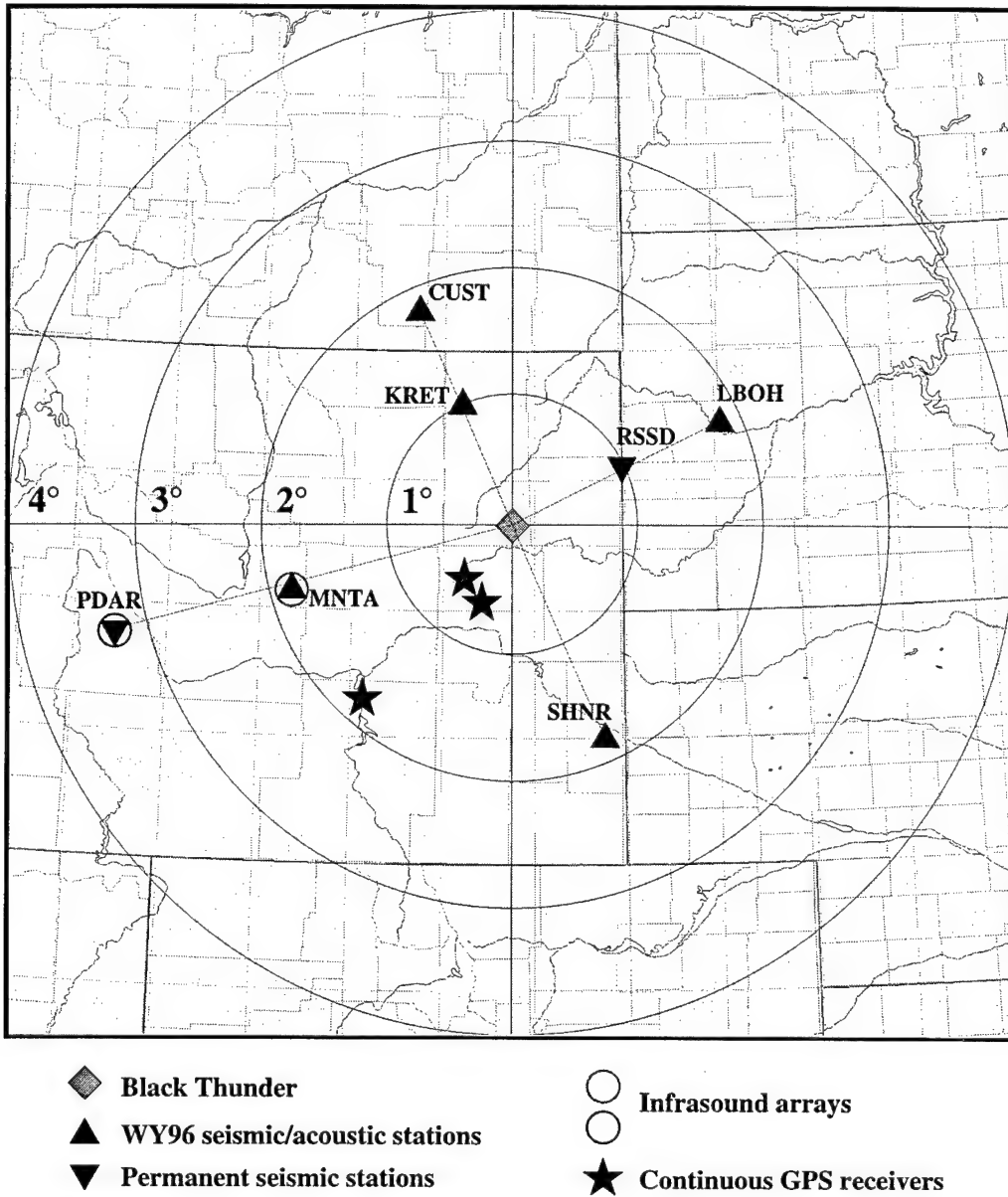


Figure 11. The 1996 Black Thunder regional deployment. The WY96 seismic stations consist of 3-Component STS2 broadband seismometers. The seismometers will be making continuous recordings digitized at 100 sps. The acoustic sensors are DNA pressure gauges. The W96 infrasound array will be deployed 200 km to the west of Black Thunder (at MNTA). This array will consist of 3 sensors arranged in a triangle.

Software contribution: An initial version of our ATFD has been given to David Jepsen at the IDC and is currently being incorporated into their Detection Feature Extraction (DFX) software package.

B. CONCLUSIONS AND PLANS FOR THE COMING YEAR

The key question which we are attempting to address with our research is: Can a robust discriminant be developed which will discriminate large numbers of industrial, multiple, explosions from nuclear explosions and earthquakes? It seems that the generic ATFD is robust with misclassification probabilities

NORESS B - a test of a vertical- and 3-Component array

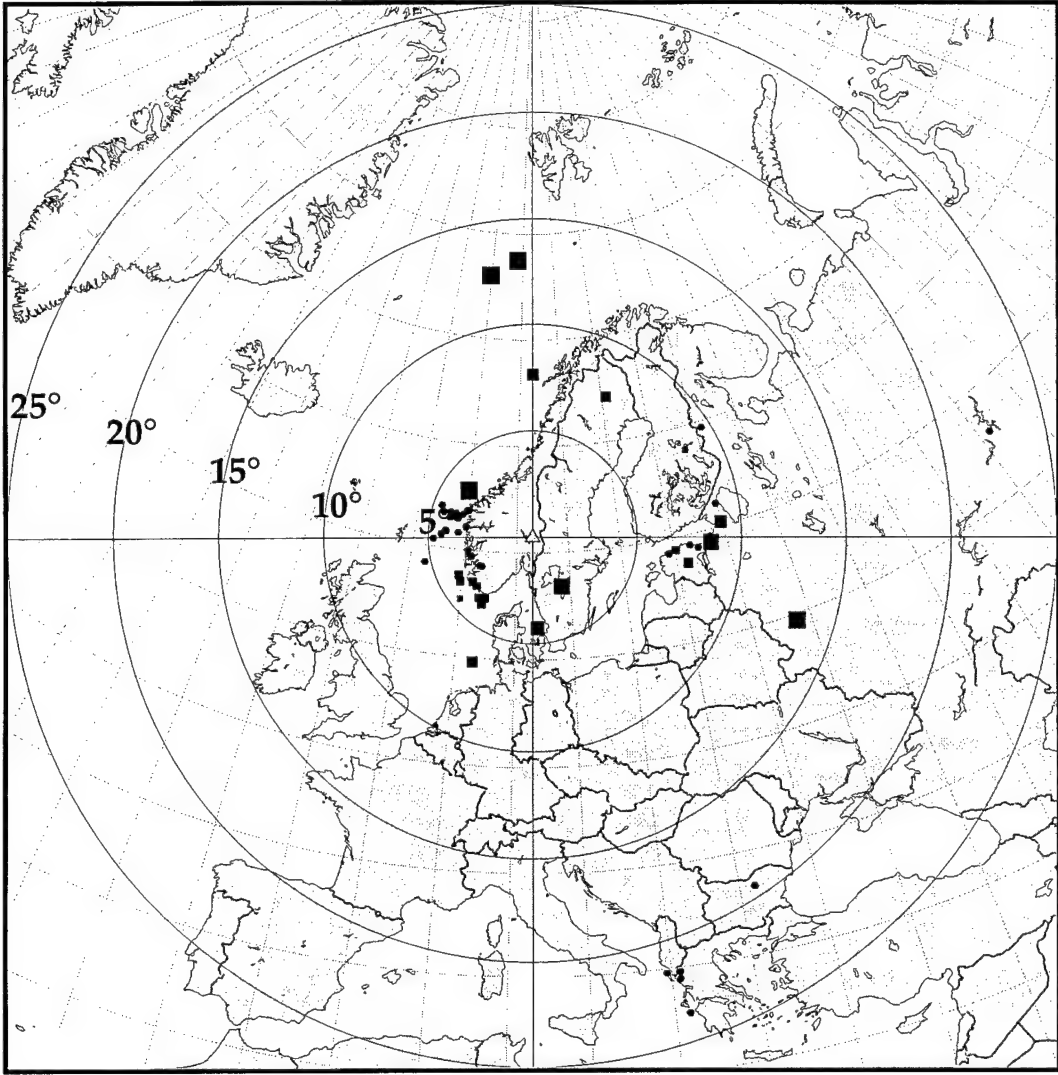


Figure 12. The NORESS B dataset. This dataset, provided to us by Jay Pulli, contains recordings of quarry blasts and earthquakes made by NORESS. Some events are located as much as 25° from the array.

ranging from 0.5 to 3.5%. The ATFD is easily adapted to a wide range of deployments (from single stations to arrays and networks) and thus easily automated. Discrimination using time-frequency expansions does not rely on expert interpretation but is routine, robust and easily automated.

In the coming year we will broaden the scope of our test of the ATFD by analyzing data at greater ranges and in regions not closely studied before:

- Examine data collected by the Saudi Network (*Vernon et al., 1996*)
- Examine CNET data
- Examine J. Pulli's NORESS Ground Truth Database to test ATFD at greater range (Figure 12).

Small-event discrimination at low frequencies. There have been a number of observations of a spectral null at low (< 10 Hz) frequencies (e.g. *Gitterman and Van Eck, 1993*) observing mines at local ranges in

Israel). A null is predicted by linear wavefield superposition and is due to source finiteness. If this is detectable in the events in the aforementioned datasets we will attempt to determine if this spectral quality can be used for discrimination at far-regional distances (> 400 km). We are currently analyzing NRDC recordings of single and multiple explosions and have made arrangements to analyze recordings made in Wyoming in 1995 by LANL, LLNL and AFTAC.

We will examine more recordings of single explosions (*e.g.* those recorded in Wyoming in 1995 by *Stump et al., 1995* and *Pearson et al., 1995*).

We will further examine wavelet based time-frequency expansions and analyze the variations of amplitude and polarization with time and frequency to better understand the genesis of seismic coda. We will bring a wavelet based ATFD on line if it proves to be superior to the existing algorithm.

We will continue our analysis of tightly constrained mining events and dual (seismic and acoustic) monitoring technology by analyzing the data collected in Wyoming this summer. With these data we will address the question of the physics of ripple-fired wavefield superposition, the range to which ripple-fired events can be detected and improve our understanding of outliers. This experiment will enable us to test the utility of continuous GPS for event detection.

C. REFERENCES

- Baumgardt, D. R. & Ziegler, K. A., 1988, Spectral Evidence for Source Multiplicity in Explosions: Application to Regional Discrimination of Earthquakes and Explosions, *Bull. Seismol. Soc. Amer.*, 78, 1773-1795.
- Daubechies, I., 1990, The wavelet transform, time-frequency localization and signal analysis, *IEEE Transactions on information theory*, 36, 961-1005.
- Gitterman, Y. & van Eck, T., 1993, Spectra of quarry blasts and microearthquakes recorded at local distances in Israel, *Bull. Seismol. Soc. Amer.*, 83, 1799-1812.
- Grant, L. & Carabajal, C., 1995, Ground-Truth Database for Regional Seismic Identification Research, *proceedings of the 17th Seismic Research Symposium*, Scottsdale, AZ, Sept 12-15, PL-TR-95-2108, ADA310037.
- Hansen, R., 1992, Research plan for the Pinedale Seismic Research Facility, AFTAC report AFTAC-TR-92-000.
- Hedlin, M.A.H., Minster, J.-B. & Orcutt, J.A., 1989, The time-frequency characteristics of quarry blasts and calibration explosions recorded in Kazakhstan, U.S.S.R., *Geophys. J. Int.*, 99, 109-121.
- Hedlin, M.A.H., Minster, J.-B. & Orcutt, J.A., 1990, An automatic means to discriminate between earthquakes and quarry blasts, *Bull. Seismol. Soc. Amer.*, 80, 2143-2160.
- Hedlin, M.A.H., Vernon, F.L., Minster, J.-B. & Orcutt, J.A., 1995, Regional Small-Event Identification using Seismic Networks and Arrays, *proceedings of the 17th Seismic Research Symposium on Monitoring a CTBT*, Scottsdale, AZ, Sept, p 875-884, PL-TR-95-2108, ADA310037.
- Lilly, J.M. & Park, J., 1995, Multiwavelet spectral and polarization analysis of seismic records, *manuscript in press with the Geophysical Journal International*.
- Park, J., Lindberg, C.R. & Vernon, F.L., Multitaper Spectral Analysis of High-Frequency Seismograms, *J. Geophys. Res.*, 92, 12675-12684.
- Pearson, D.C., Stump, B.W., Baker, D.F. & Edwards, C.L., The LANL/LLNL/AFTAC Black Thunder Mine Regional Mining Blast Experiment, *proceedings of the 17th Seismic Research Symposium on Monitoring a CTBT*, Scottsdale, AZ, Sept, p 562-571, PL-TR-95-2108, ADA310037.
- Seber, G.A.F., 1994, Multivariate Observations, Wiley series in probability and mathematical statistics, John Wiley & Sons, Inc.
- Stump, B.W., Pearson, D.C., Edwards, C.L & Baker, D.F., The LANL Source Geometry Experiment, *proceedings of the 17th Seismic Research Symposium on Monitoring a CTBT*, Scottsdale, AZ, Sept, p684-693, PL-TR-95-2108, ADA310037.

Stump, G.W., Riviere-Barbier, F., Chernobyl, I. & Koch, K., 1994, Monitoring a test ban treaty presents scientific challenges, *EOS, Trans. of the American Geophys. Union*, **75**, 265.

Thomson, D.J., 1982, Spectrum Estimation and Harmonic Analysis, *IEEE Proc.*, **70**, 1055-1096.

Thurber, C., Given, H. & Berger, J., 1989, Regional Seismic Event Location With a Sparse Network: Application to Eastern Kazakhstan, USSR, *Journal of Geophysical Research*, **94**, 17767-17780.

Tribolet, J. M., 1979, Seismic Applications of Homomorphic Signal Processing, Prentice-Hall Signal Processing Series.

Vernon, F.L., Mellors, R.J., Berger, J., Al-Amri, A.M. & Zollweg, J., 1996, Initial Results from the Deployment of Broadband Seismometers in the Saudi Arabian Shield, the proceedings of the 18th Seismic Research Symposium, Annapolis, MD, Sept 4-6, PL-TR-96-2153. **ADA313692**

Wuster, J., 1993, Discrimination of chemical explosions and earthquakes in central Europe - a case study, *Bull. Seis. Soc. Am.*, **83**, 1184-1212.

Appendix A The Automated Time-Frequency Discriminant:

We have noted (in the main body of this report and previously in *Hedlin et al., 1989*) that the frequency content of seismic onsets and coda resulting from ripple-fired explosions is often highly independent of the recording component and time. It is well known that the energy is often scalloped in frequency (*e.g. Bell & Alexander, 1977; Baumgardt & Ziegler, 1988*). These qualities are due to source finiteness, the intershot delays or a combination of the two (*Hedlin et al., 1989; 1990*). They can sometimes be acquired during propagation through a resonant crust (*Hedlin et al., 1989*).

To determine the degree to which these qualities are present in a seismic coda we first expand the recording into a time-frequency display (sonogram) by sliding a window (usually 2.5 seconds long) along the time series (with the window sliding 20% of its length each time). A spectral estimate is calculated at each window position using 7 multitapers (*Thomson, 1982; Park et al., 1987*) with a time-bandwidth product of 4. Two multitaper sonograms of recordings made during the 1987 NRDC experiment (Figure A1) are displayed in Figures A2 and A3. These were obtained from recordings of a single (chemical) explosion and a quarry blast. As described in *Hedlin et al. (1989)* each multitaper spectral estimate is converted into binary form through convolution with two boxcars (usually spanning 4.4 and 2.0 Hz), differencing the two smoothed spectra and replacing all locally high (and low) spectral values with +1 (and -1). Using the original, spectral, sonogram we estimate the average pre-onset noise level, $N(f)$, and randomize all values in the binary sonogram, $B(f,t)$, which have a smaller spectral amplitude than this average. This randomization is recorded by a mask, $R(f,t)$, which equals 1 or 0 (indicating a randomized point or one that is untouched). Noise suppression is directed at long-lived spectral lines which would, if left untouched, give a sonogram an improperly high level of time-independence. Four binary sonograms are displayed in Figure A4. The upper left pattern was obtained from a recording of a single chemical explosion (Figure A2). The other three patterns were obtained from a 3-Component recording of a quarry blast (Figure A3). This figure shows the high correlation (in time and across recording directions) of the scallops present in the binary sonograms extracted from the quarry blast.

Although the sonograms contain a wealth of information about the evolution of spectral energy in seismic coda they must be collapsed into a few parameters which are diagnostic of ripple-firing and can be used for automatic source discrimination.:

Independence from recording direction. This quality is estimated simply by calculating the zero lag cross-correlation between the three pairs of binary sonograms (vertical with east-west; vertical with north-south, north-south with east-west). Given two binary sonograms E and Z (obtained from the east-west and vertical recordings of the same event) the zero lag cross-correlation is given by:

$$X_{EZ} = \frac{\sum_{i=1}^{n_{freq}} \sum_{j=1}^{n_{time}} E(i,j)Z(i,j)R_E(i,j)R_Z(i,j)}{\sum_{i=1}^{n_{freq}} \sum_{j=1}^{n_{time}} R_E(i,j)R_Z(i,j)}$$

where R_E and R_Z are the E-W and Z randomization masks. This sum incorporates only those points which have not been randomized. The perfect correspondence of non-randomized points would yield a cross correlation of 1.0. We generally do not rotate the data into physical coordinates since this was found to yield no improvement. When multiple 3-Component recordings are available (either in a network or an array) the individual estimates (*e.g.* of the cross correlation between Z and EW) are

NRDC - A sparse 3C network

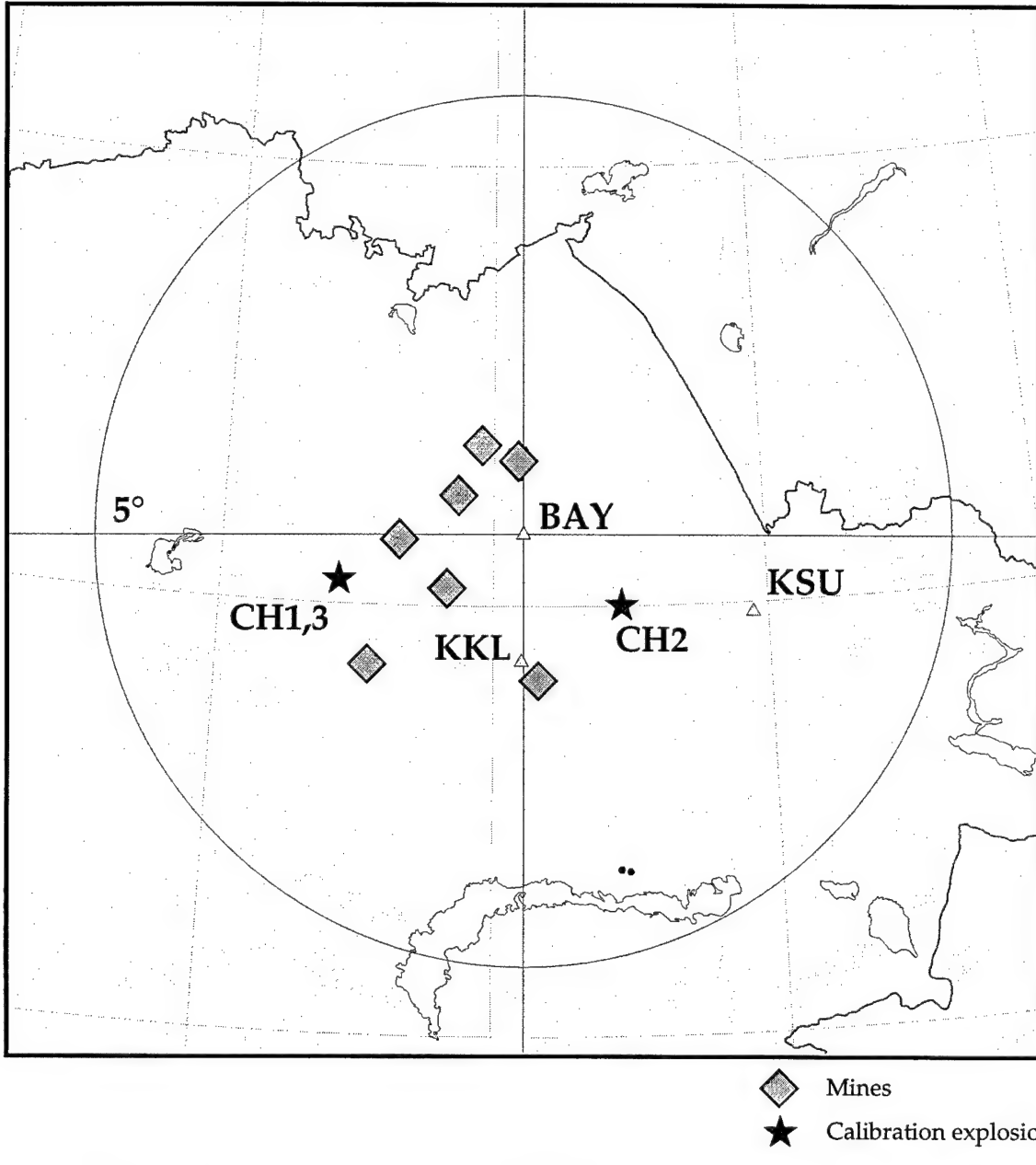


Figure A1. The NRDC network was deployed in 1987 in central Kazakhstan (see Figure 1) and collected triggered 250 sps recordings at the surface and in boreholes of three calibration explosions, numerous local and regional quarry blasts and a large number of far-regional/teleseismic earthquakes. This study is concerned with events recorded within 5° of the stations.

averaged together. Thus, regardless of the nature of the seismic 3-Component deployment, component independence yields three parameters for discrimination.

Time Independence and Periodicity in Frequency. These qualities are estimated together by using the coda cepstrum. The cepstrum is calculated by taking the Fourier transform of the log (base 10) of a single, detrended, spectral estimate (*Baumgardt & Ziegler, 1988*). The coda cepstrum (as defined by *Hedlin et al., 1995*) is calculated by taking the two-dimensional Fourier transform of the binary sonogram (which is detrended by the conversion into binary form). The two-dimensional coda cepstrum is sensitive to spectral periodicities which are constant, or cyclic, with time in the onset phases and coda. To

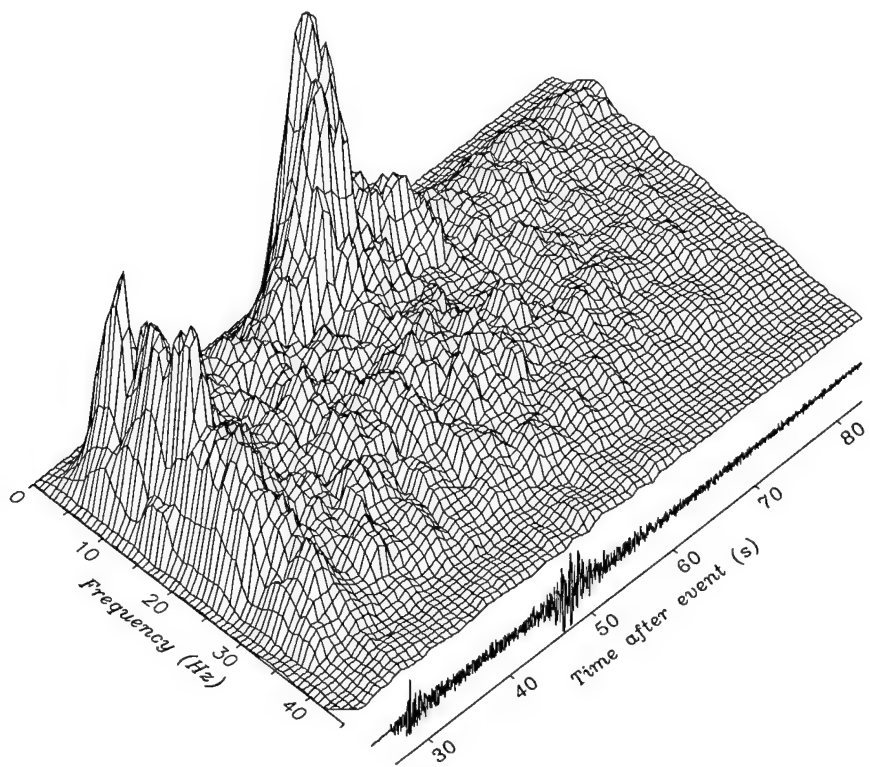


Figure A2. Seismogram resulting from a single chemical explosion (CH2; Figure A1) detonated in Kazakhstan and corresponding sonogram. The recording was made at a range of 157 km by the vertical component seismometer at Bayanaul.

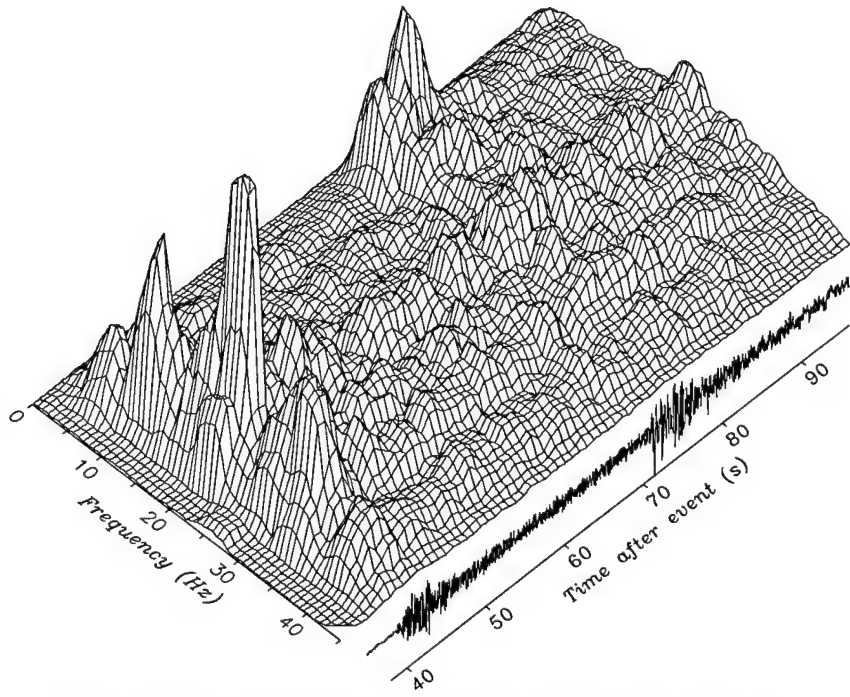


Figure A3. Seismogram resulting from a ripple-fired quarry blast (EVC; Figure A1) detonated in Kazakhstan and corresponding sonogram. The recording was made at a range of 264 km by the vertical component seismometer at Bayanaul.

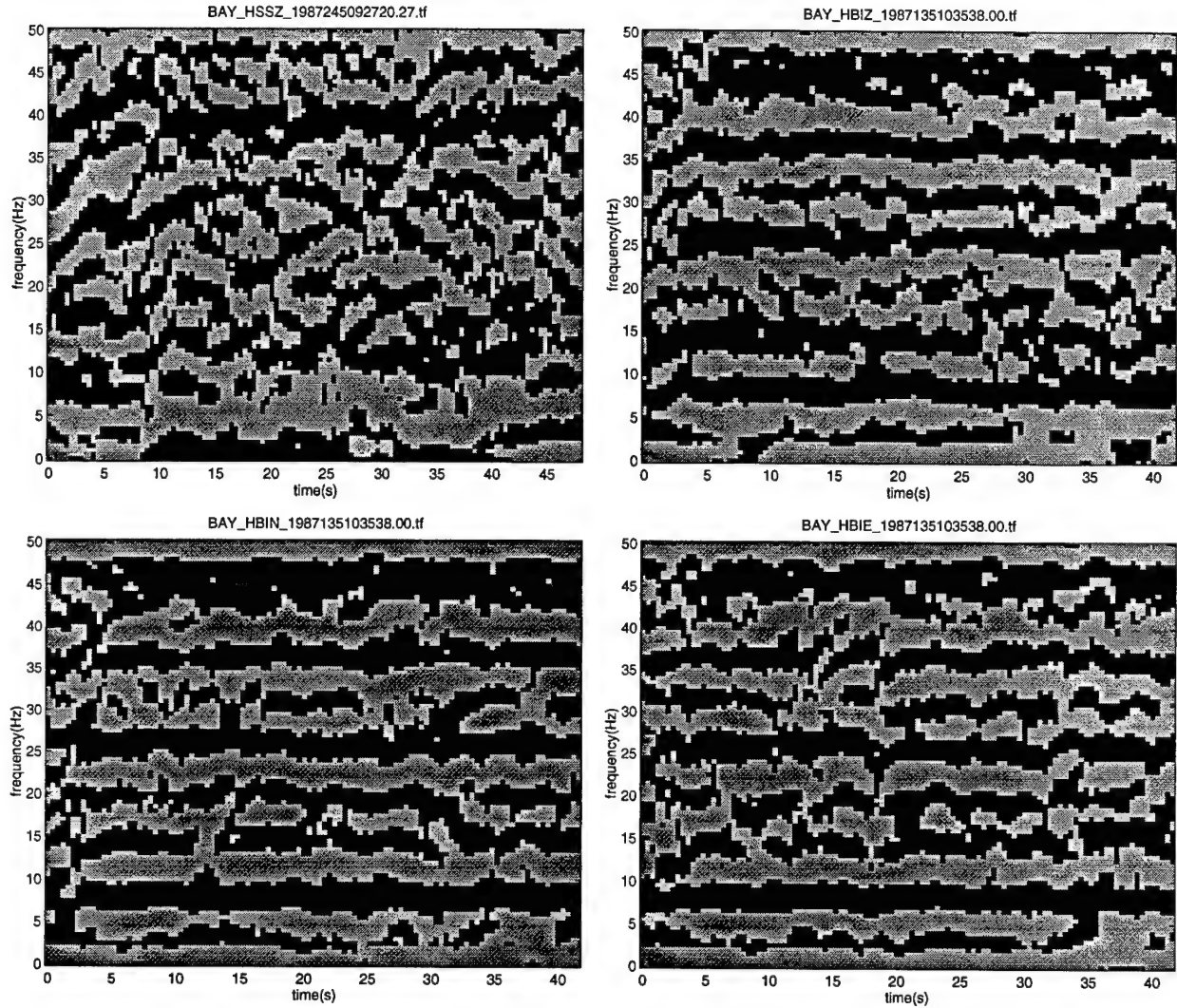


Figure A4. Binary versions of the sonograms presented in Figure B2 (upper left) and B3 (upper right). Binary sonograms calculated from the north lower (left) and east (lower right) component recordings of event c (Figures B1 and B3).

estimate the degree to which time-independent scallops are present we take the maximum of the coda cepstrum at a time-frequency of zero. This value is normalized relative to the maximum of the coda cepstrum calculated from a synthetic binary sonogram (which has the same periodicity in frequency and is independent of time with the exception that the randomization mask applied to the real sonogram is also applied to the synthetic). The quefrency of the maximum can be used to estimate a dominant ripple-fire delay or source duration. When the event has been recorded by numerous sensors, the cepstral values are averaged together. Thus, when applied to a single component deployment, the coda cepstrum will yield a single parameter. A 3-Component deployment, averaged in the same fashion, will yield three.

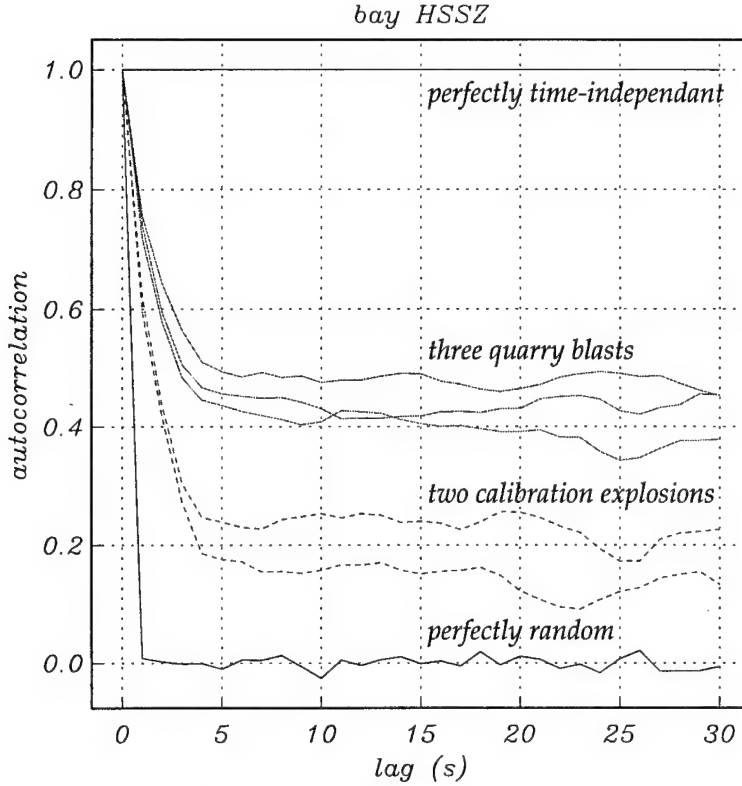


Figure A5. The autocorrelations calculated for three quarry blasts and two calibration explosions recorded during the 1987 NRDC experiment. Also plotted are the autocorrelations for synthetic sonograms that are perfectly random and one that is independent of time.

For an additional measure of time-independence we apply an autocorrelation operator to the binary matrix, $B(f,t)$, where the autocorrelation at a lag of k windows, $A(k)$, is given by:

$$A(k) = \frac{\sum_{i=1}^{n\text{freq}} \sum_{j=1}^{ntime-k} B(i,j)B(i,j+k)R(i,j)R(i,j+k)}{\sum_{i=1}^{n\text{freq}} \sum_{j=1}^{ntime-k} R(i,j)R(i,j+k)}$$

Considering events recorded by the NRDC network we have found that the autocorrelation does not depend on the lag (provided that the lags are large enough to ensure no window overlap). In practice, when using 2.5 second windows with 20% overlap, we use minimum lag of 6 windows and a maximum equal to the duration of the sonogram). All pairs which include a point that has been randomized, due to noise, are excluded. For a robust estimate of A we average over all appropriate lags. As above, autocorrelation yields a single averaged parameter (or three if the deployment has 3-Component stations).

With the measures described above the ATFD yields nine parameters when applied to a 3-Component deployment or just two (from the coda-cepstrum and autocorrelation) when single component data are available. These parameters are typically merged using multivariate statistics. The ATFD is trained in a new region by processing a number of known quarry blasts and earthquakes and/or calibration explo-

sions. In effect, the ATFD is taught to recognize the binary patterns produced by the two types of events (ripple-fired/non-ripple-fired).

Appendix B — A Global Test of the ATFD

We briefly described the results of the KNET experiment in the main body of this report. The five other studies listed in section two are briefly summarized in this appendix. These datasets were selected so that we could determine if the ATFD is easily adapted to different styles of deployment (single 3-Component station; tight array; sparse or dense 3-C network) and successfully discriminate ripple-fired events from single explosions and earthquakes in spite of varying mining practice and geologic settings. In all cases standard tests were applied to ensure the validity of the statistical analysis.

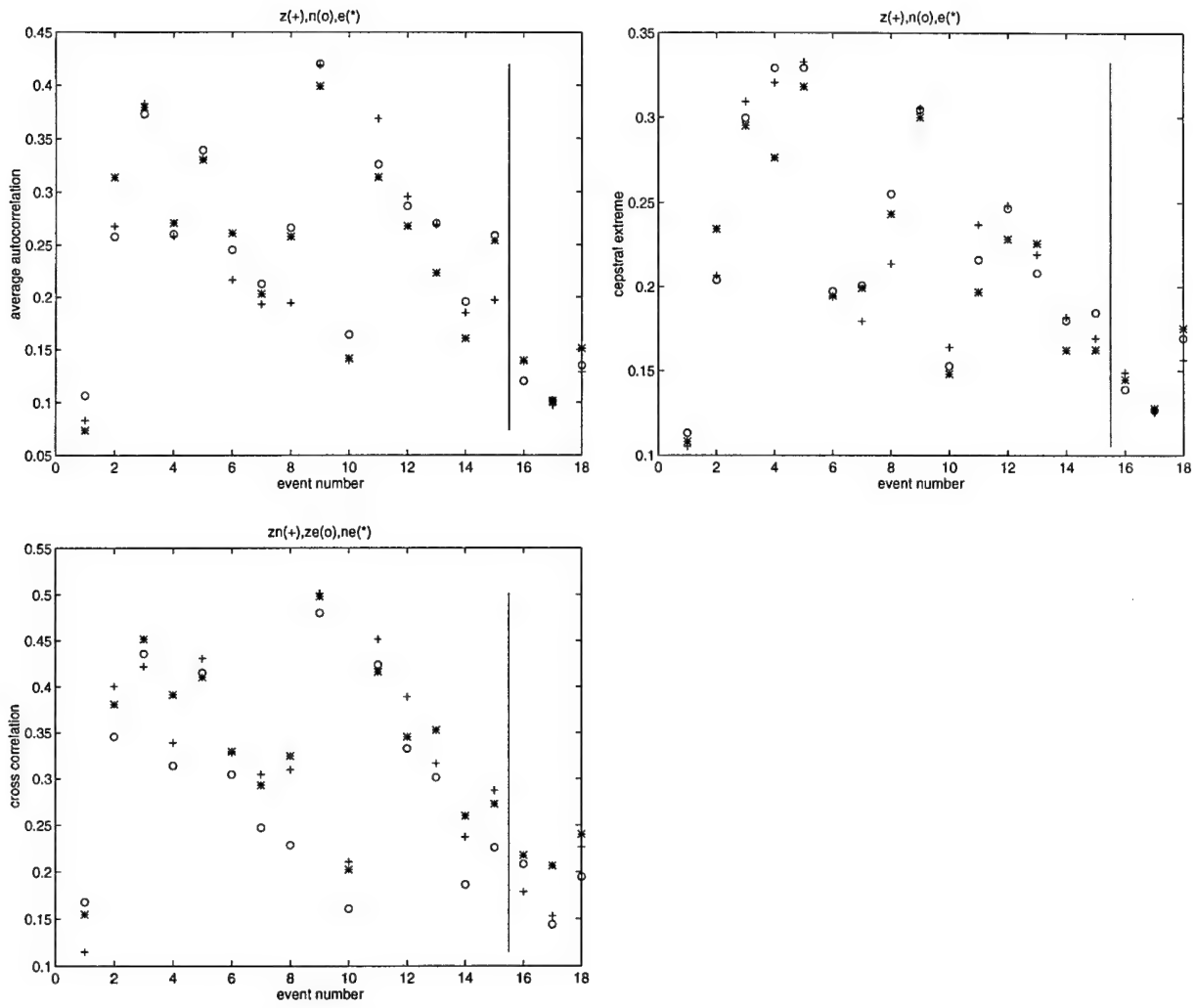
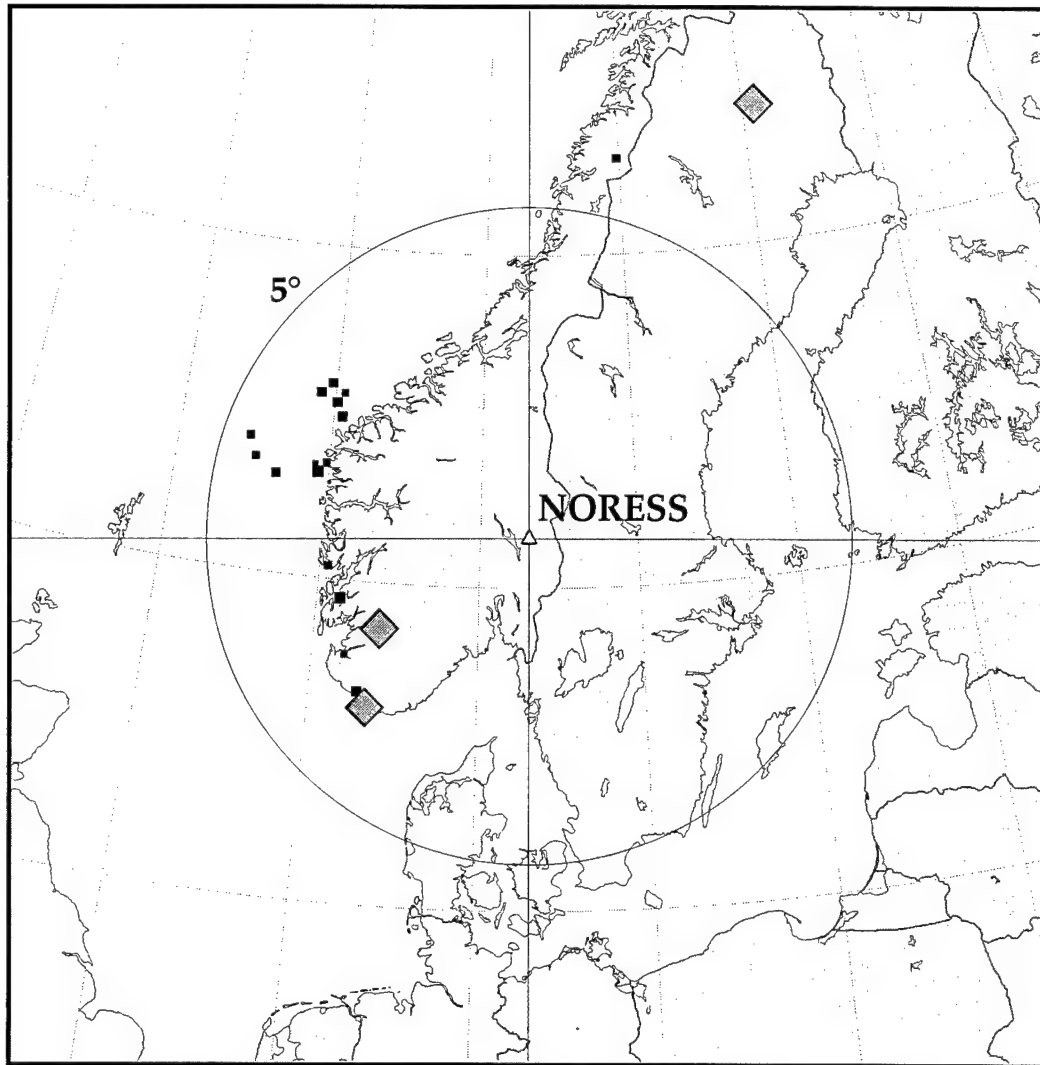


Figure B1. The three discrimination parameters (described in Appendix A) calculated using the NRDC recordings. The quarry blasts are events 1 through 15, the calibration explosions are events 16 to 18. The events, with the exception of #s 1 and 10, separate quite well. The quarry blasts are presumed to be ripple-fired.

NRDC: The 1987 NRDC experiment was unique for several reasons. Recordings of local mining activity and teleseismic natural seismicity were made in Kazakhstan, USSR, by a sparse 3-Component network situated near the Semipalatinsk nuclear test site (Figure A1). Three calibration explosions (ranging in size from 10 tons to 20 tons) were detonated during the test at regional distances from the NRDC stations. A disadvantage, from the perspective of demonstrating robustness of a discriminant, is that just 3 single-shots were recorded. We can demonstrate visually a tendency for the ATFD to be able to separate single and multiple explosions but can't support this with a statistical analysis. As a result we display, in Figure B1, the raw output from the ATFD but no multivariate statistics. What we see in this figure is a clear separation of most of the quarry blasts from the calibration events. Two events (1 and 10), which we have presumed are ripple-fired quarry blasts, are judged to be similar to the calibration events.

NORESS A - a test of a vertical- and 3-Comonent array



◆ Mines

Figure B2 Dataset number 4. Collected by the NORESS small aperture array. This dataset contains recordings of 26 quarry blasts (from 3 mines including Blasjo and Titania) and 16 earthquakes. The events range from 2.7 to 7.5° from the array and have magnitudes of 1.6 to 3.0. A preliminary analysis of these events is presented in *Hedlin et al. (1990)*.

NORESS A: The regional NORESS dataset (first analyzed by *Hedlin et al., 1990*) consists of 42 events, 26 quarry blasts and 16 earthquakes (Figure B2). As displayed in Figure B3 all statistical measures applied by the ATFD show an obvious separation of the two event types - no events were misclassified (the misclassification probability is 3.7%). This is a promising result given that one of the quarries is located 7.5° from NORESS.

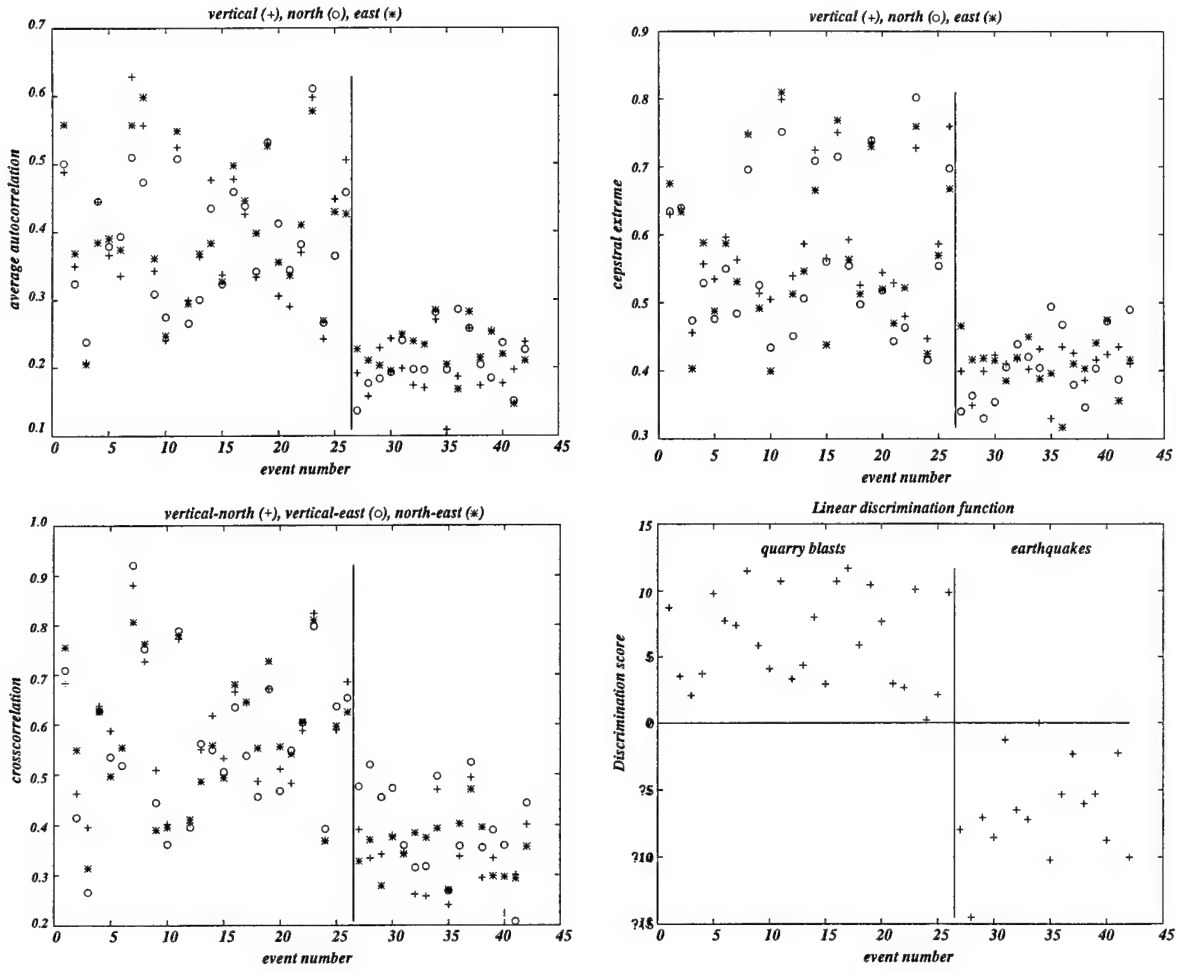


Figure B3. The four panels in this figure show the output of the ATFD applied to NORESS recordings of the events displayed in Figure B6. Events 1 through 26 are quarry blasts, 27 through 42 are earthquakes.

VOGLAND - a test of a vertical- & 3-Component array

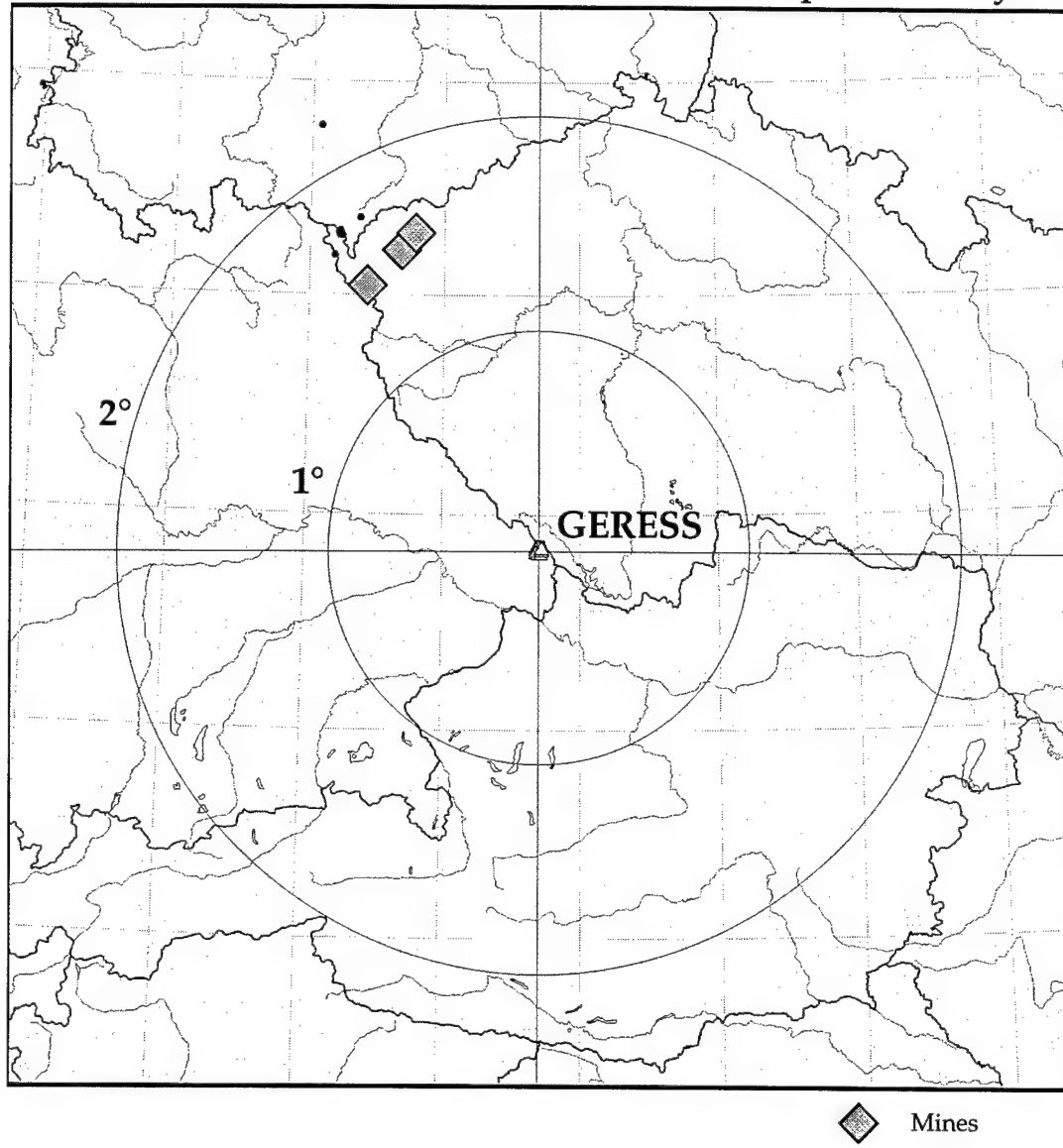


Figure B4. The Vogtland dataset was recorded by GELESS and obtained through the European Ground Truth Database. The data was contributed to this database by Jan Wuster.

Vogtland: The events in this dataset were recorded by GELESS (Figure B4). They were obtained from Jan Wuster via the European Ground Truth Database (Grant & Carabajal, 1995). Included are 11 quarry blasts and 10 earthquakes. All events are located between 1.5 and 2.5° to the northwest of the array. These populations are easily separated by the ATFD (misclassification probability of 0.55%; Figure B5).

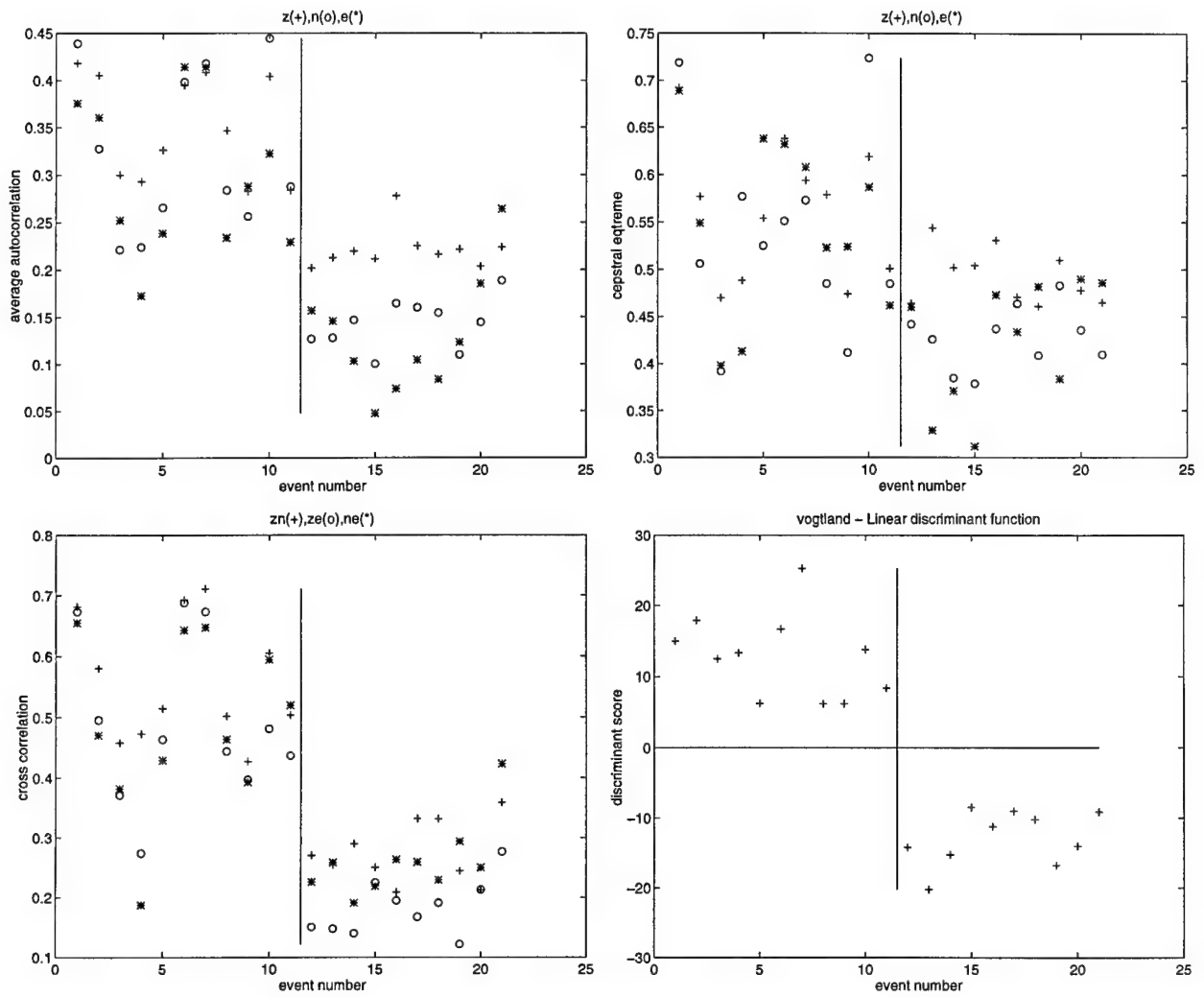
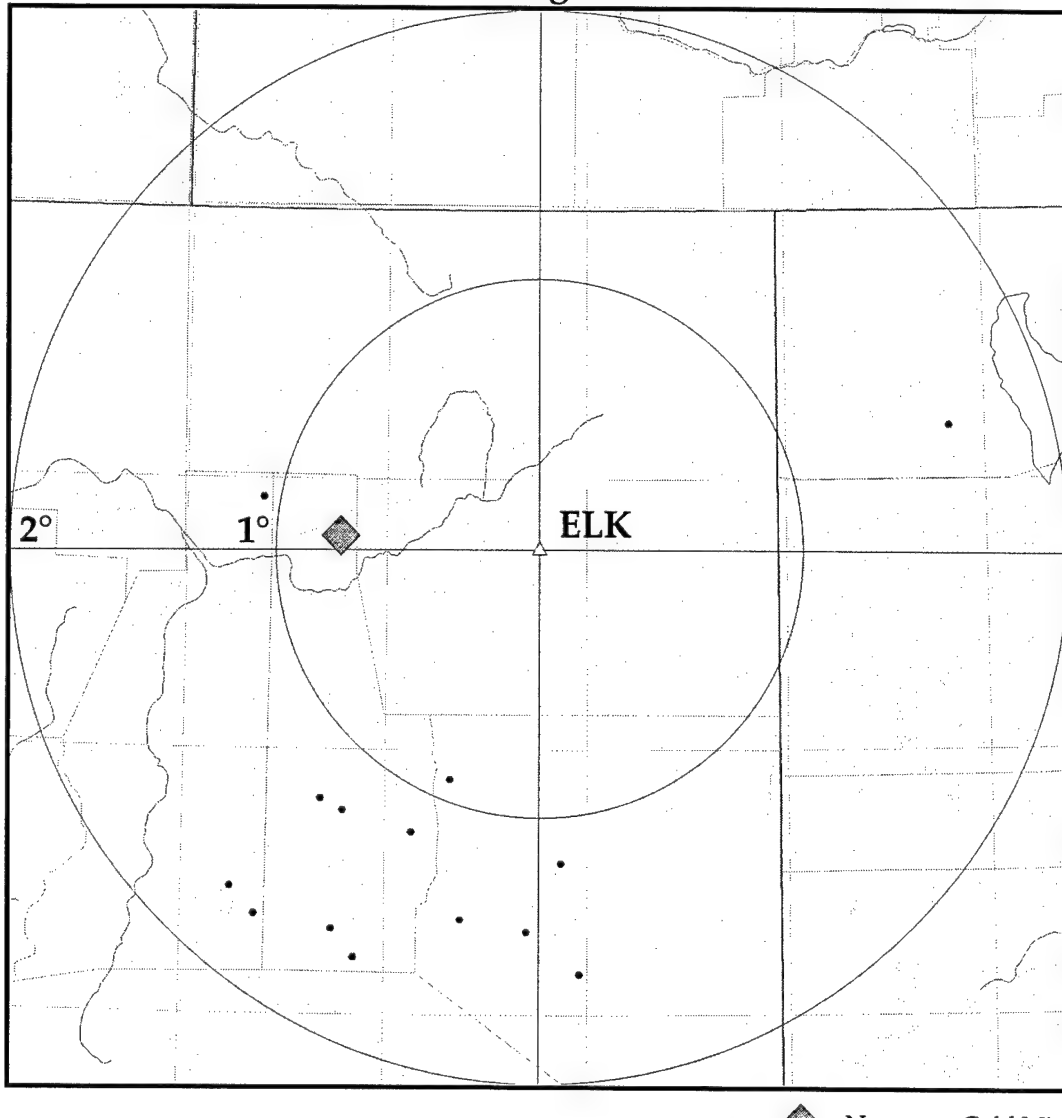


Figure B5. The Vogtland discrimination results.

Carlin - A single 3C station



◆ Newmont Gold Mine

Figure B6. The Carlin dataset includes recordings of mine blasts made at the Newmont Gold Mine in Nevada and widely distributed earthquakes. The recordings were made by a single 3-Component station (ELK). The data were provided to us by Steve Jarpe and Peter Goldstein at LLNL.

Carlin: This dataset, contributed to us by Steve Jarpe and Peter Goldstein at LLNL, consists of 42 quarry blasts (all occurring at the Newmont Gold Mine in Nevada) and 36 widely dispersed earthquakes (Figure B6). The events occurred within 2° of the single 3-Component station ELK. Again, these events are easily separated by the ATFD. Of the 78 events, just 1 was misclassified (the misclassification probability is 2.6%; Figure B7).

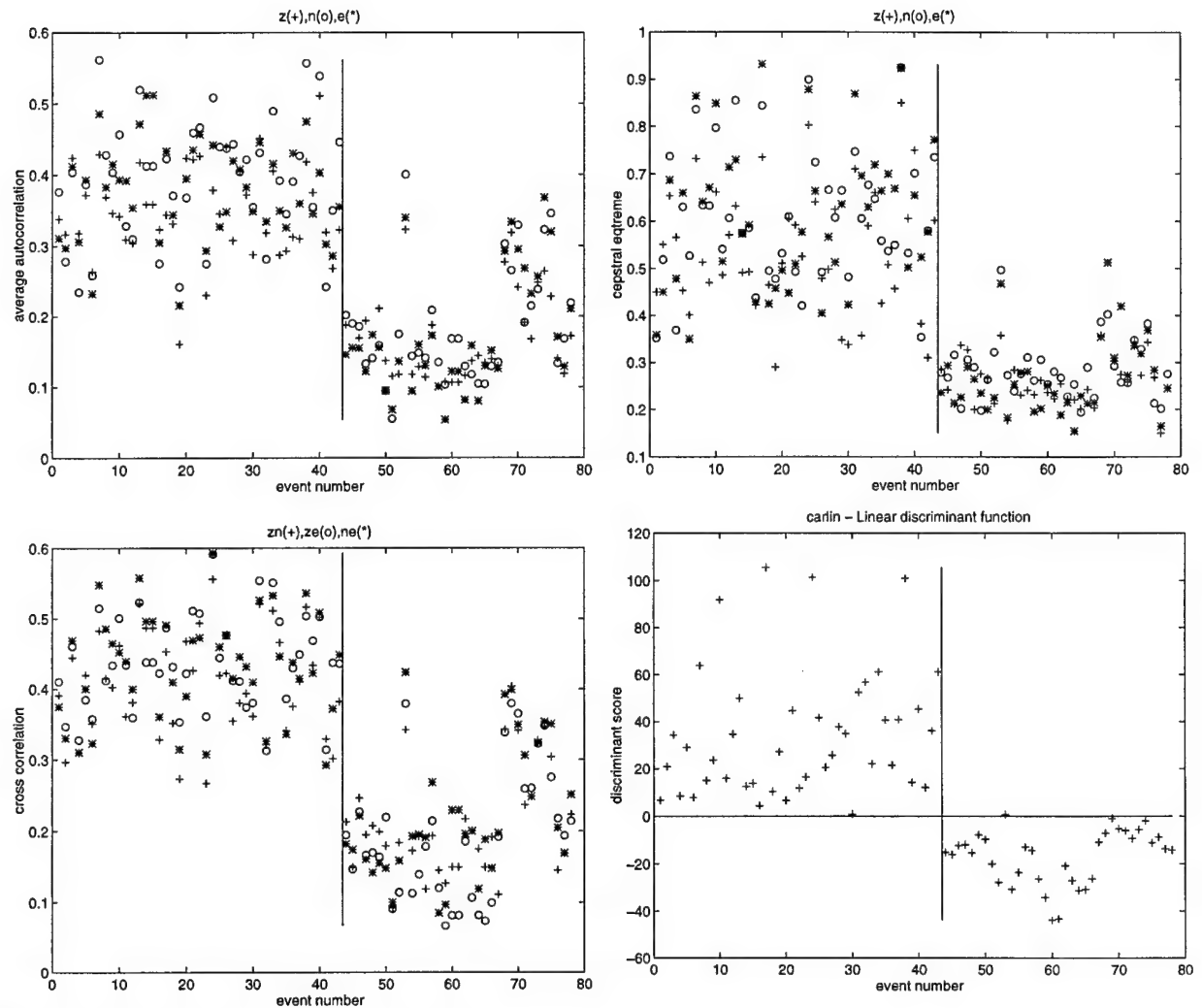


Figure B7. Carlin discrimination results.

THOMAS AHRENS
SEISMOLOGICAL LABORATORY 252-21
CALIFORNIA INSTITUTE OF TECHNOLOGY
PASADENA, CA 91125

RALPH ALEWINE
NTPO
1901 N. MOORE STREET, SUITE 609
ARLINGTON, VA 22209

SHELTON ALEXANDER
PENNSYLVANIA STATE UNIVERSITY
DEPARTMENT OF GEOSCIENCES
537 DEIKE BUILDING
UNIVERSITY PARK, PA 16801

MUAWIA BARAZANGI
INSTITUTE FOR THE STUDY OF THE CONTINENTS
3126 SNEE HALL
CORNELL UNIVERSITY
ITHACA, NY 14853

RICHARD BARDZELL
ACIS
DCI/ACIS
WASHINGTON, DC 20505

T.G. BARKER
MAXWELL TECHNOLOGIES
P.O. BOX 23558
SAN DIEGO, CA 92123

DOUGLAS BAUMGARDT
ENSCO INC.
5400 PORT ROYAL ROAD
SPRINGFIELD, VA 22151

THERON J. BENNETT
MAXWELL TECHNOLOGIES
11800 SUNRISE VALLEY DRIVE SUITE 1212
RESTON, VA 22091

WILLIAM BENSON
NAS/COS
ROOM HA372
2001 WISCONSIN AVE. NW
WASHINGTON, DC 20007

JONATHAN BERGER
UNIVERSITY OF CA, SAN DIEGO
SCRIPPS INSTITUTION OF OCEANOGRAPHY IGPP, 0225
9500 GILMAN DRIVE
LA JOLLA, CA 92093-0225

ROBERT BLANDFORD
AFTAC
1300 N. 17TH STREET
SUITE 1450
ARLINGTON, VA 22209-2308

STEVEN BRATT
NTPO
1901 N. MOORE STREET, SUITE 609
ARLINGTON, VA 22209

RHETT BUTLER
IRIS
1616 N. FORT MEYER DRIVE
SUITE 1050
ARLINGTON, VA 22209

LESLIE A. CASEY
DOE
1000 INDEPENDENCE AVE. SW
NN-40
WASHINGTON, DC 20585-0420

CATHERINE DE GROOT-HEDLIN
SCRIPPS INSTITUTION OF OCEANOGRAPHY
UNIVERSITY OF CALIFORNIA, SAN DIEGO
INSTITUTE OF GEOPHYSICS AND PLANETARY PHYSICS
LA JOLLA, CA 92093

STANLEY DICKINSON
AFOSR
110 DUNCAN AVENUE, SUITE B115
BOLLING AFB
WASHINGTON, D.C. 20332-001

SEAN DORAN
ACIS
DCI/ACIS
WASHINGTON , DC 20505

DIANE I. DOSER
DEPARTMENT OF GEOLOGICAL SCIENCES
THE UNIVERSITY OF TEXAS AT EL PASO
EL PASO, TX 79968

RICHARD J. FANTEL
BUREAU OF MINES
DEPT OF INTERIOR, BLDG 20
DENVER FEDERAL CENTER
DENVER, CO 80225

JOHN FILSON
ACIS/TMG/NTT
ROOM 6T11 NHB
WASHINGTON, DC 20505

MARK D. FISK
MISSION RESEARCH CORPORATION
735 STATE STREET
P.O. DRAWER 719
SANTA BARBARA, CA 93102-0719

LORI GRANT
MULTIMAX, INC.
311C FOREST AVE. SUITE 3
PACIFIC GROVE, CA 93950

I. N. GUPTA
MULTIMAX, INC.
1441 MCCORMICK DRIVE
LARGO, MD 20774

JAMES HAYES
NSF
4201 WILSON BLVD., ROOM 785
ARLINGTON, VA 22230

MICHAEL HEDLIN
UNIVERSITY OF CALIFORNIA, SAN DIEGO
SCRIPPS INSTITUTION OF OCEANOGRAPHY IGPP, 0225
9500 GILMAN DRIVE
LA JOLLA, CA 92093-0225

EUGENE HERRIN
SOUTHERN METHODIST UNIVERSITY
DEPARTMENT OF GEOLOGICAL SCIENCES
DALLAS, TX 75275-0395

VINDELL HSU
HQ/AFTAC/TTR
1030 S. HIGHWAY A1A
PATRICK AFB, FL 32925-3002

RONG-SONG JIH
PHILLIPS LABORATORY
EARTH SCIENCES DIVISION
29 RANDOLPH ROAD
HANSOM AFB, MA 01731-3010

LAWRENCE LIVERMORE NATIONAL LABORATORY
ATTN: TECHNICAL STAFF (PLS ROUTE)
PO BOX 808, MS L-200
LIVERMORE, CA 94551

LAWRENCE LIVERMORE NATIONAL LABORATORY
ATTN: TECHNICAL STAFF (PLS ROUTE)
PO BOX 808, MS L-221
LIVERMORE, CA 94551

ROBERT GEIL
DOE
PALAIS DES NATIONS, RM D615
GENEVA 10, SWITZERLAND

HENRY GRAY
SMU STATISTICS DEPARTMENT
P.O. BOX 750302
DALLAS, TX 75275-0302

DAVID HARKRIDER
PHILLIPS LABORATORY
EARTH SCIENCES DIVISION
29 RANDOLPH ROAD
HANSOM AFB, MA 01731-3010

THOMAS HEARN
NEW MEXICO STATE UNIVERSITY
DEPARTMENT OF PHYSICS
LAS CRUCES, NM 88003

DONALD HELMBERGER
CALIFORNIA INSTITUTE OF TECHNOLOGY
DIVISION OF GEOLOGICAL & PLANETARY SCIENCES
SEISMOLOGICAL LABORATORY
PASADENA, CA 91125

ROBERT HERRMANN
ST. LOUIS UNIVERSITY
DEPARTMENT OF EARTH & ATMOSPHERIC SCIENCES
3507 LACLEDE AVENUE
ST. LOUIS, MO 63103

ANTHONY IANNACCHIONE
BUREAU OF MINES
COCHRANE MILL ROAD
PO BOX 18070
PITTSBURGH, PA 15236-9986

THOMAS JORDAN
MASSACHUSETTS INSTITUTE OF TECHNOLOGY
EARTH, ATMOSPHERIC & PLANETARY SCIENCES
77 MASSACHUSETTS AVENUE, 54-918
CAMBRIDGE, MA 02139

LAWRENCE LIVERMORE NATIONAL LABORATORY
ATTN: TECHNICAL STAFF (PLS ROUTE)
PO BOX 808, MS L-207
LIVERMORE, CA 94551

LAWRENCE LIVERMORE NATIONAL LABORATORY
ATTN: TECHNICAL STAFF (PLS ROUTE)
LLNL
PO BOX 808, MS L-175
LIVERMORE, CA 94551

LAWRENCE LIVERMORE NATIONAL LABORATORY
ATTN: TECHNICAL STAFF (PLS ROUTE)
PO BOX 808, MS L-208
LIVERMORE, CA 94551

LAWRENCE LIVERMORE NATIONAL LABORATORY
ATTN: TECHNICAL STAFF (PLS ROUTE)
PO BOX 808, MS L-202
LIVERMORE, CA 94551

LAWRENCE LIVERMORE NATIONAL LABORATORY
ATTN: TECHNICAL STAFF (PLS ROUTE)
PO BOX 808, MS L-195
LIVERMORE, CA 94551

LAWRENCE LIVERMORE NATIONAL LABORATORY
ATTN: TECHNICAL STAFF (PLS ROUTE)
PO BOX 808, MS L-205
LIVERMORE, CA 94551

THORNE LAY
UNIVERSITY OF CALIFORNIA, SANTA CRUZ
EARTH SCIENCES DEPARTMENT
EARTH & MARINE SCIENCE BUILDING
SANTA CRUZ, CA 95064

ANATOLI L. LEVSHIN
DEPARTMENT OF PHYSICS
UNIVERSITY OF COLORADO
CAMPUS BOX 390
BOULDER, CO 80309-0309

DONALD A. LINGER
DNA
6801 TELEGRAPH ROAD
ALEXANDRIA, VA 22310

LOS ALAMOS NATIONAL LABORATORY
ATTN: TECHNICAL STAFF (PLS ROUTE)
PO BOX 1663, MS F659
LOS ALAMOS, NM 87545

LOS ALAMOS NATIONAL LABORATORY
ATTN: TECHNICAL STAFF (PLS ROUTE)
PO BOX 1663, MS F665
LOS ALAMOS, NM 87545

LOS ALAMOS NATIONAL LABORATORY
ATTN: TECHNICAL STAFF (PLS ROUTE)
PO BOX 1663, MS D460
LOS ALAMOS, NM 87545

LOS ALAMOS NATIONAL LABORATORY
ATTN: TECHNICAL STAFF (PLS ROUTE)
PO BOX 1663, MS C335
LOS ALAMOS, NM 87545

GARY MCCARTOR
SOUTHERN METHODIST UNIVERSITY
DEPARTMENT OF PHYSICS
DALLAS, TX 75275-0395

KEITH MC LAUGHLIN
MAXWELL TECHNOLOGIES
P.O. BOX 23558
SAN DIEGO, CA 92123

BRIAN MITCHELL
DEPARTMENT OF EARTH & ATMOSPHERIC SCIENCES
ST. LOUIS UNIVERSITY
3507 LACLEDE AVENUE
ST. LOUIS, MO 63103

RICHARD MORROW
USACDA/TVI
320 21ST STREET, N.W.
WASHINGTON, DC 20451

JOHN MURPHY
MAXWELL TECHNOLOGIES
11800 SUNRISE VALLEY DRIVE SUITE 1212
RESTON, VA 22091

JAMES NI
NEW MEXICO STATE UNIVERSITY
DEPARTMENT OF PHYSICS
LAS CRUCES, NM 88003

CHARLES ODDENINO
BUREAU OF MINES
810 7TH ST. NW
WASHINGTON, DC 20241

JOHN ORCUTT
INSTITUTE OF GEOPHYSICS AND PLANETARY PHYSICS
UNIVERSITY OF CALIFORNIA, SAN DIEGO
LA JOLLA, CA 92093

PACIFIC NORTHWEST NATIONAL LABORATORY
ATTN: TECHNICAL STAFF (PLS ROUTE)
PO BOX 999, MS K6-48
RICHLAND, WA 99352

PACIFIC NORTHWEST NATIONAL LABORATORY
ATTN: TECHNICAL STAFF (PLS ROUTE)
PO BOX 999, MS K7-34
RICHLAND, WA 99352

PACIFIC NORTHWEST NATIONAL LABORATORY
ATTN: TECHNICAL STAFF (PLS ROUTE)
PO BOX 999, MS K7-22
RICHLAND, WA 99352

PACIFIC NORTHWEST NATIONAL LABORATORY
ATTN: TECHNICAL STAFF (PLS ROUTE)
PO BOX 999, MS K6-84
RICHLAND, WA 99352

FRANK PILOTTE
HQ/AFTAC/TT
1030 S. HIGHWAY A1A
PATRICK AFB, FL 32925-3002

JAY PULLI
RADIX SYSTEMS, INC.
6 TAFT COURT
ROCKVILLE, MD 20850

DAVID RUSSELL
HQ AFTAC/TTR
1030 SOUTH HIGHWAY A1A
PATRICK AFB, FL 32925-3002

SANDIA NATIONAL LABORATORY
ATTN: TECHNICAL STAFF (PLS ROUTE)
DEPT. 5704
MS 0979, PO BOX 5800
ALBUQUERQUE, NM 87185-0979

SANDIA NATIONAL LABORATORY
ATTN: TECHNICAL STAFF (PLS ROUTE)
DEPT. 5791
MS 0567, PO BOX 5800
ALBUQUERQUE, NM 87185-0567

SANDIA NATIONAL LABORATORY
ATTN: TECHNICAL STAFF (PLS ROUTE)
DEPT. 5704
MS 0655, PO BOX 5800
ALBUQUERQUE, NM 87185-0655

SANDIA NATIONAL LABORATORY
ATTN: TECHNICAL STAFF (PLS ROUTE)
DEPT. 6116
MS 0750, PO BOX 5800
ALBUQUERQUE, NM 87185-0750

PACIFIC NORTHWEST NATIONAL LABORATORY
ATTN: TECHNICAL STAFF (PLS ROUTE)
PO BOX 999, MS K6-40
RICHLAND, WA 99352

PACIFIC NORTHWEST NATIONAL LABORATORY
ATTN: TECHNICAL STAFF (PLS ROUTE)
PO BOX 999, MS K5-72
RICHLAND, WA 99352

PACIFIC NORTHWEST NATIONAL LABORATORY
ATTN: TECHNICAL STAFF (PLS ROUTE)
PO BOX 999, MS K5-12
RICHLAND, WA 99352

KEITH PRIESTLEY
DEPARTMENT OF EARTH SCIENCES
UNIVERSITY OF CAMBRIDGE
MADINGLEY RISE, MADINGLEY ROAD
CAMBRIDGE, CB3 OEZ UK

PAUL RICHARDS
COLUMBIA UNIVERSITY
LAMONT-DOHERTY EARTH OBSERVATORY
PALISADES, NY 10964

CHANDAN SAIKIA
WOODWARD-CLYDE FEDERAL SERVICES
566 EL DORADO ST., SUITE 100
PASADENA, CA 91101-2560

SANDIA NATIONAL LABORATORY
ATTN: TECHNICAL STAFF (PLS ROUTE)
DEPT. 6116
MS 0750, PO BOX 5800
ALBUQUERQUE, NM 87185-0750

SANDIA NATIONAL LABORATORY
ATTN: TECHNICAL STAFF (PLS ROUTE)
DEPT. 9311
MS 1159, PO BOX 5800
ALBUQUERQUE, NM 87185-1159

SANDIA NATIONAL LABORATORY
ATTN: TECHNICAL STAFF (PLS ROUTE)
DEPT. 5736
MS 0655, PO BOX 5800
ALBUQUERQUE, NM 87185-0655

THOMAS SERENO JR.
SCIENCE APPLICATIONS INTERNATIONAL
CORPORATION
10260 CAMPUS POINT DRIVE
SAN DIEGO, CA 92121

AVI SHAPIRA
SEISMOLOGY DIVISION
THE INSTITUTE FOR PETROLEUM RESEARCH AND
GEOPHYSICS
P.O.B. 2286, NOLON 58122 ISRAEL

MATTHEW SIBOL
ENSCO, INC.
445 PINEDA COURT
MELBOURNE, FL 32940

JEFFRY STEVENS
MAXWELL TECHNOLOGIES
P.O. BOX 23558
SAN DIEGO, CA 92123

DAVID THOMAS
ISEE
29100 AURORA ROAD
CLEVELAND, OH 44139

LAWRENCE TURNBULL
ACIS
DCI/ACIS
WASHINGTON, DC 20505

FRANK VERNON
UNIVERSITY OF CALIFORNIA, SAN DIEGO
SCRIPPS INSTITUTION OF OCEANOGRAPHY IGPP, 0225
9500 GILMAN DRIVE
LA JOLLA, CA 92093-0225

DANIEL WEILL
NSF
EAR-785
4201 WILSON BLVD., ROOM 785
ARLINGTON, VA 22230

RU SHAN WU
UNIVERSITY OF CALIFORNIA SANTA CRUZ
EARTH SCIENCES DEPT.
1156 HIGH STREET
SANTA CRUZ, CA 95064

JAMES E. ZOLLWEG
BOISE STATE UNIVERSITY
GEOSCIENCES DEPT.
1910 UNIVERSITY DRIVE
BOISE, ID 83725

DEFENSE TECHNICAL INFORMATION CENTER
8725 JOHN J. KINGMAN ROAD
FT BELVOIR, VA 22060-6218 (2 COPIES)

ROBERT SHUMWAY
410 MRAK HALL
DIVISION OF STATISTICS
UNIVERSITY OF CALIFORNIA
DAVIS, CA 95616-8671

DAVID SIMPSON
IRIS
1616 N. FORT MEYER DRIVE
SUITE 1050
ARLINGTON, VA 22209

BRIAN SULLIVAN
BOSTON COLLEGE
INSTITUTE FOR SPACE RESEARCH
140 COMMONWEALTH AVENUE
CHESTNUT HILL, MA 02167

NAFI TOKSOZ
EARTH RESOURCES LABORATORY, M.I.T.
42 CARLTON STREET, E34-440
CAMBRIDGE, MA 02142

GREG VAN DER VINK
IRIS
1616 N. FORT MEYER DRIVE
SUITE 1050
ARLINGTON, VA 22209

TERRY WALLACE
UNIVERSITY OF ARIZONA
DEPARTMENT OF GEOSCIENCES
BUILDING #77
TUCSON, AZ 85721

JAMES WHITCOMB
NSF
NSF/ISC OPERATIONS/EAR-785
4201 WILSON BLVD., ROOM 785
ARLINGTON, VA 22230

JIAKANG XIE
COLUMBIA UNIVERSITY
LAMONT DOHERTY EARTH OBSERVATORY
ROUTE 9W
PALISADES, NY 10964

OFFICE OF THE SECRETARY OF DEFENSE
DDR&E
WASHINGTON, DC 20330

TACTEC
BATTELLE MEMORIAL INSTITUTE
505 KING AVENUE
COLUMBUS, OH 43201 (FINAL REPORT)

PHILLIPS LABORATORY
ATTN: XPG
29 RANDOLPH ROAD
HANSCOM AFB, MA 01731-3010

PHILLIPS LABORATORY
ATTN: TSML
5 WRIGHT STREET
HANSCOM AFB, MA 01731-3004

PHILLIPS LABORATORY
ATTN: GPE
29 RANDOLPH ROAD
HANSCOM AFB, MA 01731-3010

PHILLIPS LABORATORY
ATTN: PL/SUL
3550 ABERDEEN AVE SE
KIRTLAND, NM 87117-5776 (2 COPIES)